

Quantum network theory

Bernard Yurke

AT&T Bell Laboratories, Murray Hill, New Jersey 07974

John S. Denker

Laboratory of Atomic and Solid State Physics, Cornell University, Ithaca, New York 14853

(Received 25 August 1983)

A general approach, within the framework of canonical quantization, is described for analyzing the quantum behavior of complicated electronic circuits. This approach is capable of dealing with electrical networks having nonlinear or dissipative elements. The techniques are applied to circuits capable of generating squeezed-state or two-photon coherent-state signals. Circuits capable of performing back-action-evading electrical measurements are also discussed.

I. INTRODUCTION

Quantum-mechanical considerations are playing an increasing role in the design of low-noise electromechanical networks. Recent interest in the quantum behavior of networks constructed out of discrete components has been driven by two sources: The first arose out of the practical need in experimental gravitational physics for extremely sensitive detectors operating in the quantum regime in order to measure, for example, the response of a Weber bar antenna to a passing gravitational wave from a supernova explosion in the Virgo cluster of galaxies. Out of such considerations by Braginsky, Gifford, Unruh, Caves *et al.*, and Hollenhorst arose novel concepts in measurement.¹ One of these concepts "back-action evasion" is the realization that a detector can, under suitable conditions, be made blind to its own noise.² The other major source of recent interest in the quantum behavior of electronic circuits arose out of Josephson-junction-device physics. Josephson-junction technology has reached the point where dc superconducting quantum interference devices³ and superconductor-insulator-superconductor (SIS) junction mixers⁴ are operating close to the regime where the quantum nature of the electrical signals begins to matter. The effects of dissipation on the quantum behavior of macroscopic systems has been addressed theoretically by Caldeira and Leggett,⁵ Koch *et al.*⁶ and Chakravarty.⁷ Experimental observations on electronic circuits operated in a regime where quantum noise is important have been carried out by Voss and Webb,⁸ Koch *et al.*⁹ and Jackel *et al.*¹⁰

Here we present a general approach for calculating the quantum behavior of an electromechanical network. For simplicity, the discussion is restricted to electrical networks, the generalization to other networks being straightforward. In treating dissipative elements such as resistors we follow Nyquist¹¹ and replace the resistors with transmission lines extending to infinity. This trick converts a dissipative electrical network into a manifestly conservative one and reduces the problem of quantizing the circuit to that of quantizing two-dimensional interact-

ing fields. Since the fields propagating along a transmission line satisfy a massless scalar Klein-Gordon equation, quantization is readily achieved following the standard procedures for canonical quantization. The approach presented is phenomenological in that a conservative model for an electronic circuit is constructed which correctly reproduces the classical behavior of the device. It is this model that is quantized. One may ask whether such an approach will adequately describe the behavior of a device constructed out of electrons and nucleons, i.e., would a full first-principles analysis of the 10^{23} particles making up a real electronic circuit give the same result as an approach based on macroscopic phenomenology? The attitude taken here is that the charges and magnetic fluxes stored in various components of an electronic circuit represent collective coordinates describing the cooperative motion of large numbers of electrons and that these coordinates can be quantized directly. Furthermore, thermodynamics requires that the equilibrium noise coming from a resistor depends only on the resistance R and the temperature T of the resistor. This independence of the equilibrium behavior of a resistor from its material properties or microscopic structure justifies the use of a transmission line to model the resistor.¹¹ This approach, based on classical phenomenology, will neglect electrical noise of microscopic or nonequilibrium origin such as, for example, flicker or $1/f$ noise. On the other hand, one feels that there is nothing fundamental requiring the presence of such noise sources. With proper care in engineering and fabrication, these noise sources can often be greatly reduced or eliminated. Thus the approach presented treats only that noise which is required by thermodynamics and by the Heisenberg uncertainty principles, noise of fundamental origin that cannot be engineered away by the proper choice of materials. The question addressed is the following: Given a device with a prescribed classical behavior, what is its ideal quantum performance? Hence the calculations presented here are somewhat like those of equilibrium thermodynamics. The calculations tell us what the best performance is that can be achieved by a given device. The performance of a real device is always

worse, being degraded by flicker noise and other forms of nonequilibrium noise whose origin for the most part is not well understood. However, recent advances in Josephson-junction technology^{3,4,8-10} make one optimistic that electronic circuits can indeed be built with a performance closely approaching the quantum ideal. Much of what is described here has been worked out in quantum optics. In fact, quantum network theory is simply the low-frequency limit of quantum optics. In this limit one has the luxury of working with lumped circuit components rather than distributed media. In the discussion we will try to follow the language of the electrical engineer. Kirchhoff's circuit laws turn out to be the correct Heisenberg equations of motion, provided that the appropriate current or voltage noise terms arising from the equilibrium noise coming out of the resistors are included. Hence much of classical electrical engineering can readily be carried over into the quantum domain.

Before giving a general discussion of how to quantize electrical networks, the quantum mechanics of a transmission line will be briefly reviewed in order to establish notation and present results that will be useful later when the transmission lines are used here as models of resistors. After giving a general discussion of how to carry out canonical quantization on an electrical network, the simple case of a series *LRC* circuit will be worked out in detail. The results of calculations for more complicated networks, such as those for parametric amplifiers and back-action-evasion devices, will be discussed. A simple Josephson-junction circuit is used to illustrate that certain resistive nonlinearities can also be readily handled within the framework described here. Time-dependent resistors also can be dealt with readily. An extreme case, that of a switch which has either zero or infinite resistance, is used to illustrate how one can go about calculating the ideal quantum performance of resistive mixers.

II. TRANSMISSION LINES

The quantum mechanics of transmission lines has been presented by Robinson¹² and Louisell,¹³ and is reviewed here to introduce notation, to present results that will be useful in later sections of this paper, and to make the paper self-contained. Also, some Heisenberg uncertainty relations for signals propagating along a transmission line are derived. These will be useful in discussing phase sensitive signal detection schemes.

Consider a transmission line extending to infinity in both directions along the *x* axis. Let $Q(x,t)$ denote the total charge to the right of point *x* at time *t*. $Q(x,t)$ will be referred to as the charge field. The current flowing along the transmission line is then

$$I(x,t) = \frac{\partial Q(x,t)}{\partial t}. \quad (2.1)$$

The voltage along the transmission line is given by

$$V(x,t) = -C_T^{-1} \frac{\partial Q(x,t)}{\partial x}, \quad (2.2)$$

where C_T is the capacitance per unit length along the

transmission line. The wave equation for the charge field can be obtained from the Lagrangian density

$$\mathcal{L} = \frac{1}{2} \left[L_T \left(\frac{\partial Q}{\partial t} \right)^2 - \frac{1}{C_T} \left(\frac{\partial Q}{\partial x} \right)^2 \right], \quad (2.3)$$

where L_T is the inductance per unit length along the transmission line. The wave equation is a massless scalar Klein-Gordon equation:

$$L_T \frac{\partial^2 Q}{\partial t^2} - C_T^{-1} \frac{\partial^2 Q}{\partial x^2} = 0. \quad (2.4)$$

From the Lagrangian density (2.3) the momentum $\Phi(x,t)$ canonically conjugate to the charge field can be identified:

$$\Phi(x,t) \equiv \frac{\partial L}{\partial (\partial_t Q)} = L_T I(x,t). \quad (2.5)$$

Hence $\Phi(x,t)$ is simply the magnetic flux per unit length threading the transmission line at *x* and *t*.

According to the procedure for canonical quantization,¹⁴ Q and Φ become operators satisfying the equal-time commutation relations:

$$\begin{aligned} [Q(x,t), Q(x',t)] &= [\Phi(x,t), \Phi(x',t)] = 0, \\ [Q(x,t), \Phi(x',t)] &= i\hbar \delta(x-x'). \end{aligned} \quad (2.6)$$

Since the charge field satisfies the wave equation (2.4) it can be decomposed into a left-traveling part and a right-traveling part:

$$Q(x,t) = Q_L(x/v+t) + Q_R(-x/v+t), \quad (2.7)$$

where

$$v = (L_T C_T)^{-1/2} \quad (2.8)$$

is the velocity of propagation of a signal along the transmission line. The operators Q_L and Q_R can be Fourier expanded as

$$\begin{aligned} Q_L(x/v+t) &= \left[\frac{\hbar}{4\pi Z} \right]^{1/2} \\ &\times \int_0^\infty d\omega \omega^{-1/2} (A_{L\omega} e^{-i\omega(x/v+t)} + \text{H.c.}), \end{aligned} \quad (2.9)$$

$$\begin{aligned} Q_R(-x/v+t) &= \left[\frac{\hbar}{4\pi Z} \right]^{1/2} \\ &\times \int_0^\infty d\omega \omega^{-1/2} (A_{R\omega} e^{-i\omega(-x/v+t)} \\ &\quad + \text{H.c.}), \end{aligned}$$

where

$$Z = \left[\frac{L_T}{C_T} \right]^{1/2} \quad (2.10)$$

is the characteristic impedance of the transmission line. The operators $A_{L\omega}$ and $A_{R\omega}$ are annihilation operators for signal quanta propagating, respectively, to the left or to the right. They satisfy the commutation relations

$$[A_{\alpha\omega}, A_{\alpha'\omega'}] = 0, \quad (2.11)$$

$$[A_{\alpha\omega}, A_{\alpha'\omega'}^\dagger] = \delta(\omega - \omega') \delta_{\alpha\alpha'};$$

where the index α takes on the value L or R . From (2.9) and (2.2) the voltage operator for the signal propagating to the right is given by

$$V_R(-x/v + t) = - \left[\frac{\hbar Z}{4\pi} \right]^{1/2} \times \int_B d\omega \omega^{1/2} (iA_{R\omega} e^{-i\omega(-x/v+t)} + \text{H.c.}), \quad (2.12)$$

where the integration has been limited to the bandwidth B of the measuring instrument. For the vacuum state, V_R and V_R^2 have the expectation values

$$\langle 0 | V_R | 0 \rangle = 0, \quad (2.13)$$

$$\langle 0 | V_R^2 | 0 \rangle = Z \int_B \frac{d\omega}{2\pi} \frac{\hbar\omega}{2}. \quad (2.14)$$

Hence even for the vacuum state there is $\frac{1}{2}\hbar\omega$ noise power per unit bandwidth in the zero-point fluctuations propagating to the right along the transmission line.

It will be useful, for later reference, to decompose V_R into components

$$V_R(t) = V_1(t)\cos(\omega_0 t) + V_2(t)\sin(\omega_0 t), \quad (2.15)$$

where for simplicity we have set $x=0$. V_1 and V_2 are given by

$$V_1(t) = - \left[\frac{\hbar Z}{4\pi} \right]^{1/2} \int_B d\omega \omega^{1/2} (iA_{R\omega} e^{-i(\omega-\omega_0)t} + \text{H.c.}), \quad (2.16)$$

$$V_2(t) = - \left[\frac{\hbar Z}{4\pi} \right]^{1/2} \int_B d\omega \omega^{1/2} (A_{R\omega} e^{-i(\omega-\omega_0)t} + \text{H.c.}).$$

One then can derive the following Heisenberg uncertainty relations:¹³

$$\Delta V_1(t) \Delta V_2(t') \geq \frac{\hbar Z}{4\pi} \left| \int_B d\omega \omega \cos[(\omega - \omega_0)(t - t')] \right|, \quad (2.17)$$

$$\Delta V_1(t) \Delta V_2(t') \geq \frac{\hbar Z}{4\pi} \left| \int_B d\omega \omega \sin[(\omega - \omega_0)(t - t')] \right|. \quad (2.18)$$

Setting $t=t'$ in (2.17), one has

$$\Delta V_1(t) \Delta V_2(t) \geq Z \int_B \frac{d\omega}{2\pi} \frac{\hbar\omega}{2}. \quad (2.19)$$

This places a restriction on the precision with which the components V_1 and V_2 of an electrical signal can be measured. One can show that the vacuum state is a minimum uncertainty state for relation (2.19).

III. QUANTIZING AN ELECTRICAL NETWORK, A GENERAL OVERVIEW

Figure 1(a) is a circuit diagram for a parametric amplifier. Besides the linear reactances (inductors and capacitors) and the nonlinear capacitance C_γ , the circuit has dissipative elements: the resistors R_S , R_I , and R_P . As shown in Fig. 1(b), this dissipative network can be made manifestly conservative by replacing each resistor with lossless transmission lines of infinite extent having a characteristic impedance equal to the resistance of the replaced resistor. The transmission line acts as a sink into which power can be radiated. The voltage sources in the original circuit can be replaced by signals propagating in from infinity along the transmission line. If the signals propagating in along the transmission line consist of thermal noise, then the transmission line acts as a heat bath into which the discrete components dump their energy as they thermalize with the transmission line.

Having replaced the resistors with transmission lines, the resulting manifestly conservative system can be quantized following the standard procedures of canonical quantization.¹⁴ The Lagrangian density of the system is of the form

$$\mathcal{L} = \delta(x)L + H(x) \sum_i \mathcal{L}_i, \quad (3.1)$$

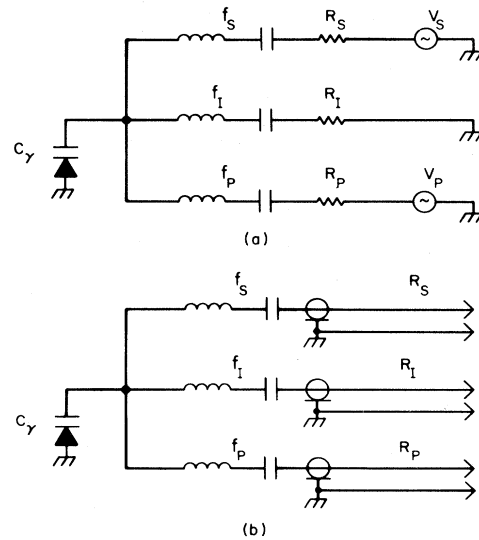


FIG. 1. (a) Circuit for a parametric amplifier. (b) The same circuit with the resistors replaced with transmission lines extending to infinity.

where L contains all the terms associated with the lumped circuit components, which are envisioned as being located at $x=0$, and $\delta(x)$ is the Dirac δ function. Terms for typical components that would be included in L are listed in Table I. The Lagrangian density for the i th transmission line is

$$\mathcal{L}_i = \frac{L_i^T}{2} \left[\frac{\partial Q_i}{\partial t} \right]^2 - \frac{1}{2C_i^T} \left[\frac{\partial Q_i}{\partial x} \right]^2, \quad (3.2)$$

where L_i^T and C_i^T are, respectively, the inductance and capacitance per unit length along the transmission line. The Heaviside function

$$H(x) = \begin{cases} 1, & x \geq 0 \\ 0, & \text{otherwise} \end{cases}$$

ensures that the transmission line only exists along the positive x axis.

The equations of motion are obtained by finding the extremum of the action

$$A = \int_{t_1}^{t_2} dt \int dx \mathcal{L}. \quad (3.3)$$



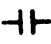
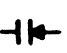
The variation of the action must however be carried out with the constraint that the total current flowing into a given electrical node be zero. That is if there are k nodes in the circuit, then one has k equations of the form

$$\sum_{\mathcal{O}} \frac{dQ_i}{dt} = 0, \quad (3.4)$$

where \mathcal{O} denotes that the sum is carried out over all the currents i entering node m . These equations simply impose the conservation of charge and are known as Kirchoff's current law. Equations (3.4) let one express all the charges in a network in terms of a set of linearly independent charges Q_i .

For simplicity, the discussion now will be restricted to linear networks with a topology sufficiently simple that the Q_i of each transmission line is linearly independent. The Lagrangian density can then be written in the form

TABLE I. Some commonly occurring circuit elements and the associated terms in the Lagrangian.

Symbol	Term in Lagrangian	Device
	$\frac{L}{2} \left[\frac{dQ}{dt} \right]^2$	linear inductance
	$M \frac{dQ_1}{dt} \frac{dQ_2}{dt}$	mutual inductance
	$-\frac{Q^2}{2C}$	linear capacitance
	$-\frac{Q^2}{2C} - \frac{\gamma Q^3}{3} + \dots$	nonlinear capacitance (varactor diode)

$$\mathcal{L} = \delta(x) \sum_{i,j} \left[\frac{L_{ij}}{2} \frac{\partial Q_i}{\partial t} \frac{\partial Q_j}{\partial t} - \frac{1}{2C_{ij}} Q_i Q_j \right] + H(x) \sum_i \left[\frac{L_i^T}{2} \left[\frac{\partial Q_i}{\partial t} \right]^2 - \frac{1}{2C_i^T} \left[\frac{\partial Q_i}{\partial x} \right]^2 \right]. \quad (3.5)$$

The procedures to be described easily can be generalized to treat networks with nonlinear elements and more complicated topologies. The variation of the action with respect to Q_i then gives the Euler-Lagrange equation

$$\frac{\partial}{\partial t} \left[\frac{\partial \mathcal{L}}{\partial (\partial_t Q_i)} \right] + \frac{\partial}{\partial x} \left[\frac{\partial \mathcal{L}}{\partial (\partial_x Q_i)} \right] - \frac{\partial \mathcal{L}}{\partial Q_i} = 0. \quad (3.6)$$

The momentum Φ_i canonically conjugate to the field variable Q_i can be identified from (3.5) via

$$\Phi_i \equiv \frac{\partial \mathcal{L}}{\partial (\partial_t Q_i)}. \quad (3.7)$$

Canonical quantization imposes the commutation relations

$$\begin{aligned} [Q_i(x,t), Q_j(x',t)] &= 0, \\ [\Phi_i(x,t), \Phi_j(x',t)] &= 0, \\ [Q_i(x,t), \Phi_j(x',t)] &= i\hbar \delta_{ij} \delta(x-x'), \end{aligned} \quad (3.8)$$

on the Q_i and Φ_i .

The $Q_i(x,t)$ can be expanded in terms of creation and annihilation operators for the transmission line fields. Quantization is then completed by introducing a vacuum state $|0\rangle$.

We now demonstrate that the terms in square brackets in Eq. (3.5) which arise from the transmission lines do indeed give linear damping as required of a resistor. The results obtained will be used to demonstrate how one can go about computing the scattering matrix for an electronic circuit. For simplicity, a system constructed out of linear circuit elements will be considered. Equation (3.5) substituted into (3.7) gives rise to the equation of motion:

$$\delta(x) \sum_j \left[L_{ij} \frac{\partial^2 Q_j}{\partial t^2} + \frac{Q_j}{C_{ij}} \right] + H(x) L_i^T \frac{\partial^2 Q_i}{\partial t^2} - \frac{1}{C_i^T} \frac{\partial}{\partial x} H(x) \frac{\partial Q_i}{\partial x} = 0. \quad (3.9)$$

For $x > 0$ this reduces to the wave equation for the i th transmission line

$$L_i^T \frac{\partial^2 Q_i}{\partial t^2} - \frac{1}{C_i^T} \frac{\partial^2 Q_i}{\partial x^2} = 0. \quad (3.10)$$

Integrating (3.9) over the interval $-\epsilon \leq x \leq \epsilon$ and taking the limit $\epsilon \rightarrow 0$ one obtains

$$\sum_j \left[L_{ij} \frac{d^2 Q_j}{dt^2} + \frac{Q_j}{C_{ij}} \right] - \frac{1}{C_i^T} \frac{\partial Q_i}{\partial x} \Big|_{x=0^+} = 0. \quad (3.11)$$

The terms in the parentheses can be recognized as the voltages developed across the inductors and capacitors. The last term is recognized from (2.2) as the voltage

across the terminals of the transmission line. Hence (3.11) is a statement of Kirchhoff's voltage law that the sum of the voltages around a closed loop is zero. Since Q_i satisfies the wave equation (3.10), it has the general form

$$Q_i(x,t) = Q_i^{\text{in}} \left[\frac{x}{v_i} + t \right] + Q_i^{\text{out}} \left[-\frac{x}{v_i} + t \right], \quad (3.12)$$

where the superscripts "in" and "out" indicate whether the signal is propagating toward the network at $x=0$ or away from it. From the time and space derivatives of (3.12), one can show that at $x=0$

$$-\frac{1}{C_i^T} \frac{\partial Q_i}{\partial x} \Big|_{x=0^+} = R_i \left[\frac{dQ_i}{dt} - 2 \frac{dQ_i^{\text{in}}}{dt} \right], \quad (3.13)$$

where R_i is the characteristic impedance of the i th transmission line (assumed to be purely resistive). Hence (3.11) becomes

$$\sum_j \left[L_{ij} \frac{d^2 Q_j}{dt^2} + \frac{Q_j}{C_{ij}} \right] + R_i \frac{dQ_i}{dt} = 2R_i \frac{dQ_i^{\text{in}}}{dt}. \quad (3.14)$$

The last term on the left side of this equation represents the voltage developed across the transmission line as the circuit radiates power into it. It is Ohm's law. The term on the right represents the voltage developed across the transmission line due to signals or noise propagating in towards the electrical network at $x=0$. This is a derivation of the fluctuation dissipation theorem for the class of networks being considered. Equation (3.14) is referred to as a Langevin equation.¹⁵ By virtue of its derivation from the Lagrangian density, (3.14) is the correct Heisenberg equation of motion. Furthermore, from (2.9) one knows how to express the Q_i^{in} in terms of $A_i^{\text{in}\dagger}(\omega)$ and $A_i^{\text{in}}(\omega)$, the creation and annihilation operators of the incoming transmission line quanta,

$$Q_i^{\text{in}}(t) = \left[\frac{\hbar}{4\pi R_i} \right]^{1/2} \int_0^\infty d\omega \omega^{-1/2} [A_i^{\text{in}}(\omega) e^{-i\omega t} + \text{H.c.}]. \quad (3.15)$$

The system of equations (3.14) can be solved for the Q_i in terms of the Q_i^{in} . From (3.12) one obtains

$$Q_i^{\text{out}} = Q_i - Q_i^{\text{in}}. \quad (3.16)$$

Hence Q_i^{out} can be expressed in terms of the Q_j^{in} . Consequently, $A_i^{\text{out}\dagger}(\omega)$ and $A_i^{\text{out}}(\omega)$, the creation and annihilation operators of outgoing quanta, can be expressed in terms of the incoming creation and annihilation operators. For the linear system considered above, one will have

$$A_i^{\text{out}}(\omega) = \sum_j S_{ij} A_j^{\text{in}}(\omega). \quad (3.17)$$

This constitutes the construction of the quantum-mechanical scattering matrix S_{ij} for the network.

Expectation values of all observable operators can now be computed for state vectors describing the incoming signals. This procedure, in the following sections, will be illustrated by discussing various electrical networks in detail. The first network to be treated will be the series *LRC* circuit.

Before moving on, it is worth describing an alternate way of coupling a transmission line to a network which has the advantage of being generalizable to model nonlinear and time-dependent dissipation. Consider the Lagrangian density

$$\begin{aligned} \mathcal{L} = & \delta(x) \sum_{i,j} \left[\frac{L_{ij}}{2} \frac{\partial Q_i}{\partial t} \frac{\partial Q_j}{\partial t} - \frac{1}{2C_{ij}} Q_i Q_j \right] \\ & + \delta(x) \sum_i T_i Q_i \frac{\partial q_i}{\partial t} \\ & + H(x) \sum_i \left[\frac{L_i^T}{2} \left(\frac{\partial q_i}{\partial t} \right)^2 - \frac{1}{2C_i^T} \left(\frac{\partial q_i}{\partial x} \right)^2 \right]. \end{aligned} \quad (3.18)$$

In contrast to (3.5), the i th transmission line, instead of being hooked directly into the circuit, is coupled to the i th charge Q_i via the linear coupling $T_i Q_i dq_i/dt$.

It now will be demonstrated that such a coupling gives rise to linear damping. In Secs. VII and VIII generalizations of this coupling will be used to model nonlinear and time-dependent resistors. The Euler-Lagrange equations for (3.18) yield for $x=0$

$$\sum_j \left[L_{ij} \frac{d^2 Q_j}{dt^2} + \frac{Q_j}{C_{ij}} \right] - T_i \frac{dq_i}{dt} = 0, \quad (3.19)$$

$$T_i \frac{dQ_i}{dt} - \frac{1}{C_i^T} \frac{\partial q_i}{\partial x} \Big|_{x=0^+} = 0, \quad (3.20)$$

and for $x > 0$

$$L_i^T \frac{\partial^2 q_i}{\partial t^2} - \frac{1}{C_i^T} \frac{\partial^2 q_i}{\partial x^2} = 0. \quad (3.21)$$

Let the impedance of the i th transmission line be denoted as Z_i , then in analogy with (3.13) one has

$$-\frac{1}{C_i^T} \frac{\partial q_i}{\partial x} \Big|_{x=0^+} = Z_i \left[\frac{dq_i}{dt} - 2 \frac{dq_i^{\text{in}}}{dt} \right] \quad (3.22)$$

and q_i^{in} has the form of (3.15)

$$q_i^{\text{in}}(t) = \left[\frac{\hbar}{4\pi Z_i} \right] \int_0^\infty d\omega \omega^{-1/2} [A_i^{\text{in}}(\omega) e^{-i\omega t} + \text{H.c.}]. \quad (3.23)$$

With (3.20) and (3.22), Eq. (3.19) can be reexpressed as

$$\sum_j \left[L_{ij} \frac{d^2 Q_j}{dt^2} + \frac{Q_j}{C_{ij}} \right] + R_i \frac{dQ_i}{dt} = 2T_i \frac{dq_i^{\text{in}}}{dt}, \quad (3.24)$$

where the resistance R_i is given by

$$R_i = T_i^2 / Z_i. \quad (3.25)$$

That the coupling $T_i Q_i dq_i/dt$ gives rise to linear damping has now been demonstrated with the appearance of the term $R_i dQ_i/dt$ in Eq. (3.24). If one introduces an effective charge Q_i^{in} via the definition

$$Q_i^{\text{in}} \equiv \frac{Z_i}{T_i} q_i^{\text{in}}, \quad (3.26)$$

Eq. (3.24) can be reexpressed to be identical with (3.14). Furthermore, by substituting (3.23) into (3.26) one can show that the expression for the effective charge Q_i^{in} is identical with (3.15). Hence it has been demonstrated that the Lagrangian densities (3.5) and (3.18) lead to the same dynamical behavior as far as the Q_i 's are concerned. This is reassuring since thermodynamics requires that the equilibrium noise developed across a resistor be characterized only by the temperature and resistance of a resistor. The equilibrium behavior of a resistor should be independent of how the resistor is constructed. The model one uses to simulate a resistor is a matter of convenience. Simulating a resistor by replacing it with a transmission line leads to a very simple Lagrangian density. On the other hand, the coupling in the Lagrangian density (3.18) is more readily generalized to treat nonlinear and time-dependent dissipation.

IV. THE SERIES LRC CIRCUIT

A number of approaches to the quantum mechanics of the damped harmonic oscillator have been proposed. These have been extensively reviewed by Dekker.¹⁶ Our approach is in the spirit of Senitzky,¹⁷ Ford *et al.*,¹⁸ and more recently Caldeira and Leggett⁵ in that a simple heat bath (a transmission line in our case) is coupled to the oscillator to produce the damping. Figure 2(a) depicts a driven, damped series LRC circuit. Figure 2(b) is the same circuit in which the resistor and voltage source have been replaced with a transmission line of infinite extent. The Lagrangian density for the system is

$$\mathcal{L} = \delta(x) \left[\frac{L}{2} \left[\frac{\partial Q}{\partial t} \right]^2 - \frac{Q^2}{2C} \right] + H(x) \left[\frac{L_T}{2} \left[\frac{\partial Q}{\partial t} \right]^2 - \frac{1}{2C_T} \left[\frac{\partial Q}{\partial x} \right]^2 \right]. \quad (4.1)$$

The Euler-Lagrange equation, following the same steps that lead to Eq. (3.14), yields

$$L \frac{d^2 Q}{dt^2} + R \frac{dQ}{dt} + \frac{Q}{C} = 2R \frac{dQ^{\text{in}}}{dt}. \quad (4.2)$$

Since this equation is linear and since Q^{in} has the form (3.15), one readily can solve for Q in terms of $A_{\text{in}}^{\dagger}(\omega)$ and $A_{\text{in}}(\omega)$, the creation and annihilation operators of the incoming charge field. The result is

$$Q(t) = \left[\frac{\hbar R}{\pi} \right]^{1/2} \int_0^{\infty} d\omega \omega^{1/2} \left[\frac{i A_{\text{in}}(\omega) e^{-i\omega t}}{\omega^2 L - 1/C + i\omega R} + \text{H.c.} \right]. \quad (4.3)$$

From (3.16), the signal propagating back out along the transmission line is

$$Q_{\text{out}}(t) = \left[\frac{\hbar}{4\pi R} \right]^{1/2} \int_0^{\infty} d\omega \omega^{-1/2} [A_{\text{out}}(\omega) e^{-i\omega t} + \text{H.c.}], \quad (4.4)$$

where

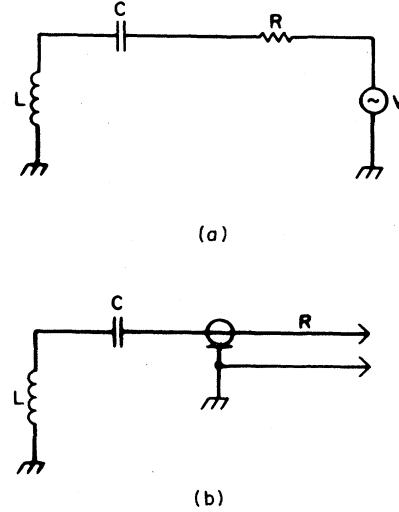


FIG. 2. (a) A damped, driven series LRC circuit. (b) The same circuit with the resistor and voltage source replaced with a transmission line.

$$A_{\text{out}}(\omega) = - \frac{\omega^2 L - 1/C - i\omega R}{\omega^2 L - 1/C + i\omega R} A_{\text{in}}(\omega). \quad (4.5)$$

Remembering from Eq. (2.11) that

$$[A_{\text{in}}(\omega), A_{\text{in}}(\omega')] = 0, \quad (4.6)$$

$$[A_{\text{in}}(\omega), A_{\text{in}}^{\dagger}(\omega')] = \delta(\omega - \omega'),$$

it is an easy exercise in contour integration to demonstrate that

$$\left[Q, L \frac{dQ}{dt} \right] = i\hbar. \quad (4.7)$$

This is the electrical equivalent of $[x, p] = i\hbar$. Equations (4.1)–(4.6) constitute a complete solution of the quantum LRC problem. The expectation values of the operators for various incoming signals can now be computed. Suppose the resistor is at absolute zero, $T=0$, then only vacuum fluctuations will come out of the resistor. Hence the signal propagating in along the transmission line is modeled by the state vector $|0\rangle$ defined by

$$A_{\text{in}}(\omega) |0\rangle = 0 \quad \text{for all } \omega. \quad (4.8)$$

It is instructive to work out the probability distribution $P(q)$ for finding an amount of charge q in the capacitor. One can show

$$\langle 0 | Q(t) | 0 \rangle = 0$$

and

$$\langle \Delta Q \rangle^2 = \langle 0 | Q^2(t) | 0 \rangle = \frac{\hbar}{\pi R} \int_0^{\infty} \frac{\omega}{\omega^2 + \frac{L^2}{R^2}(\omega^2 - \omega_0^2)} d\omega, \quad (4.9)$$

where

$$\omega_0 = (LC)^{-1/2}.$$

The higher-order moments are given by

$$\begin{aligned} \langle 0 | Q^{2k} | 0 \rangle &= (2k-1)!! \langle 0 | Q^2 | 0 \rangle^k, \\ \langle 0 | Q^{2k+1} | 0 \rangle &= 0. \end{aligned} \quad (4.10)$$

From (4.9) and (4.10) one can conclude that the probability distribution is Gaussian¹⁹

$$P(q) = (2\pi)^{-1/2} (\Delta Q)^{-1} e^{-q^2/2(\Delta Q)^2}. \quad (4.11)$$

The integration in (4.9) can be carried out and the result is

$$(\Delta Q)^2 = \frac{\hbar}{\pi} \left[\frac{C}{L} \right]^{1/2} \frac{\mathcal{Q}}{(4\mathcal{Q}^2-1)^{1/2}} \cot^{-1} \left[-\frac{2\mathcal{Q}^2-1}{(4\mathcal{Q}^2-1)^{1/2}} \right], \quad \mathcal{Q} > \frac{1}{2} \quad (4.12a)$$

$$(\Delta Q)^2 = \frac{\hbar}{\pi} \left[\frac{C}{L} \right]^{1/2}, \quad \mathcal{Q} = \frac{1}{2} \quad (4.12b)$$

$$\frac{\hbar}{2\pi} \left[\frac{C}{L} \right]^{1/2} \frac{\mathcal{Q}}{(1-4\mathcal{Q}^2)^{1/2}} \ln \left[\frac{1-2\mathcal{Q}^2+(1-4\mathcal{Q}^2)^{1/2}}{1-2\mathcal{Q}^2-(1-4\mathcal{Q}^2)^{1/2}} \right], \quad \mathcal{Q} < \frac{1}{2} \quad (4.12c)$$

where \mathcal{Q} is the quality factor

$$\mathcal{Q} = \frac{L\omega_0}{R}. \quad (4.13)$$

The three cases (4.12a), (4.12b), and (4.12c) correspond, respectively, to the underdamped, critically damped, and overdamped LRC oscillator. In the limit when the quality factor \mathcal{Q} becomes unbounded ($\mathcal{Q} \rightarrow \infty$), one finds

$$(\Delta Q)^2 = \frac{\hbar}{2} \left[\frac{C}{L} \right]^{1/2}.$$

For the mechanical analog, $L \rightarrow M$, $1/C \rightarrow K$, and $Q \rightarrow x$, one has

$$(\Delta x)^2 = \left[\frac{\hbar^2}{4MK} \right]^{1/2}$$

which is the textbook result for the undamped harmonic oscillator. It can be seen from Eqs. (4.12a)–(4.12c) that the width of the charge distribution becomes narrower as the damping is increased. This has observable consequences for the macroscopic quantum tunneling rates of Josephson junctions.^{5,8–10}

V. PARAMETRIC AMPLIFIERS

The restrictions quantum mechanics places on the performance of linear amplifiers were first worked out in the 1950s when the advent of the maser, an amplifier capable of extremely low noise operation, made such considerations of practical importance. The history of interest in the quantum limits of linear amplifiers is briefly reviewed by Caves²⁰ and the reader is directed there for references. As Caves has pointed out, it is necessary to distinguish between phase insensitive and phase sensitive linear amplifiers. Let the voltage V_{in} of a signal with a narrow band about ω_0 be written in component form as

$$V_{in}(t) = V_1(t)\cos(\omega_0 t) + V_2(t)\sin(\omega_0 t), \quad (5.1)$$

where ω_0 can be regarded as a clock or reference frequency. Suppose that when this signal is fed into the amplifier, the amplified output voltage can be written in the form

$$\begin{aligned} V_{out}(t) &= A_1 V_1(t)\cos(\omega_0 t + \phi) \\ &+ A_2 V_2(t)\sin(\omega_0 t + \phi). \end{aligned} \quad (5.2)$$

The amplifier will be referred to as being phase insensitive if $A_1 = A_2$. In most literature such amplifiers are simply referred to as linear amplifiers. If $A_1 \neq A_2$ the amplifier will be referred to as phase sensitive. It is a well-known result that a linear phase insensitive amplifier must add noise to the amplified signal. A phase sensitive linear amplifier, in contrast, under suitable conditions can be completely noise free. An example of a phase sensitive amplifier is the degenerate parametric amplifier (DPA) which Takahasi²¹ in (1965) recognized could be in principle noise-free quantum mechanically. A derivation of the quantum performance of a DPA will be presented here. It is shown that the DPA performs a canonical transformation on the signals delivered to its input and this transformation is completely reversible. (A second DPA can undo what the first DPA has done.) The techniques described can be extended to treat nondegenerate parametric amplifiers and upconverters. Towards the end of this section some comments will be made about phase insensitive linear amplifiers. In particular, it will be shown that phase insensitive amplifiers in principle can be built which can noiselessly amplify one component of a signal. Hence the commonly asserted claim that a phase insensitive linear amplifier must inject noise into the amplified signal with a noise power of $\frac{1}{2}\hbar\omega$ per unit bandwidth needs to be qualified to a larger extent than has been realized in the literature.

An embodiment²² of a DPA operating in the negative resistance reflection mode is shown in Fig. 3. A circulator labeled C is used to separate the input signal from the amplified output. The pump supply V_P oscillates at twice the signal frequency. Mixing of the pump and signal volt-

ages by the nonlinear capacitor C_γ makes it possible for the device to deliver net power at the signal frequency. The charge-voltage relationship for the nonlinear capacitor will be taken to be

$$V = \frac{Q}{C} + \gamma Q^2. \quad (5.3)$$

$$\begin{aligned} \mathcal{L} = & \delta(x) \left[\frac{L_S}{2} \left[\frac{\partial Q_S}{\partial t} \right]^2 + \frac{L_P}{2} \left[\frac{\partial Q_P}{\partial t} \right]^2 - \frac{Q_S^2}{2C_S} - \frac{Q_P^2}{2C_P} - \frac{(Q_S + Q_P)^2}{2C} - \frac{\gamma}{3} (Q_S + Q_P)^3 \right] \\ & + H(x) \left[\frac{L_S^T}{2} \left[\frac{\partial Q_S}{\partial t} \right]^2 - \frac{1}{2C_S^T} \left[\frac{\partial Q_S}{\partial x} \right]^2 + \frac{L_P^T}{2} \left[\frac{\partial Q_P}{\partial t} \right]^2 - \frac{1}{2C_P^T} \left[\frac{\partial Q_P}{\partial x} \right]^2 \right]. \end{aligned} \quad (5.4)$$

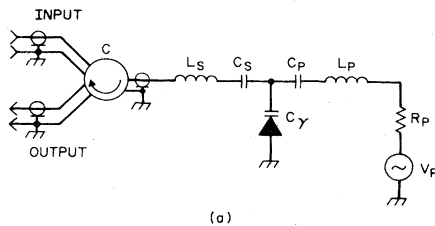
The Heisenberg equations of motion become

$$L_S \frac{d^2 Q_S}{dt^2} + R_S \frac{dQ_S}{dt} + \left[\frac{1}{C_S} + \frac{1}{C} \right] Q_S + \frac{Q_P}{C} + \gamma (Q_S + Q_P)^2 = 2R_S \frac{dQ_S^{\text{in}}}{dt}, \quad (5.5a)$$

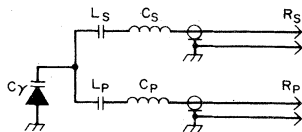
$$L_P \frac{d^2 Q_P}{dt^2} + R_P \frac{dQ_P}{dt} + \left[\frac{1}{C_S} + \frac{1}{C} \right] Q_P + \frac{Q_S}{C} + \gamma (Q_S + Q_P)^2 = 2R_P \frac{dQ_P^{\text{in}}}{dt}. \quad (5.5b)$$

Let ω_S^0 and ω_P^0 denote, respectively, the center frequencies of the LC filters of the signal and pump branch of the DPA. The assumption is now made that the quality factor of the LC filter of the signal branch is sufficiently sharp that only terms in Eq. (5.5a) oscillating at frequencies in a narrow band about ω_S^0 need be kept. A similar assumption is made for the LC filter in the pump branch of the circuit. Fourier expanding $Q_S^{\text{in}}, Q_P^{\text{in}}, Q_P$ in the form

$$Q_S^{\text{in}}(t) = \int_0^\infty d\omega [Q_S^{\text{in}}(\omega) e^{-i\omega_S t} + Q_S^{\text{in}\dagger}(\omega) e^{i\omega_S t}] \quad (5.6)$$



(a)



(b)

FIG. 3. (a) A degenerate parametric amplifier operating in the negative-resistance reflection mode. (b) A manifestly conservative version of the DPA.

For the purpose of analyzing the performance of the DPA, the circuit of Fig. 3(a) can be simplified to that of Fig. 3(b). The signal will propagate towards the amplifier along the transmission line R_S . The amplified signal will propagate out along R_S . The Lagrangian density for the circuit is

then for signals ω_S and ω_P near the resonant frequencies ω_S^0 and ω_P^0 , one obtains

$$\begin{aligned} -i\omega_S R_S Q_S(\omega_S) + \gamma \int d\omega_P [Q_P(\omega_P) Q_S^{\dagger}(\omega_P - \omega_S) \\ + Q_S^{\dagger}(\omega_P - \omega_S) Q_P(\omega_P)] \\ = -i2\omega_S R_S Q_S^{\text{in}}(\omega_S), \end{aligned} \quad (5.7a)$$

$$\begin{aligned} -i\omega_P R_P Q_P(\omega_P) + \gamma \int d\omega_S Q_S(\omega_S) Q_S(\omega_P - \omega_S) \\ = -i2\omega_P R_P Q_P^{\text{in}}(\omega_P). \end{aligned} \quad (5.7b)$$

To further simplify the problem, the limit of a weak nonlinearity ($\gamma \rightarrow 0$) will be considered. The limit will be taken in such a way that $\gamma |Q_P| = \text{const}$ where $|Q_P|$ is the amplitude of the pump. To consider what happens quantum mechanically in this limit, let the incoming pump signal be described by the Glauber state

$$\begin{aligned} |G, \gamma, \alpha\rangle = \exp \left[-\frac{1}{2\gamma^2} \int_0^\infty |\alpha(\omega)|^2 d\omega \right] \\ \times \sum_{n=0}^{\infty} \frac{1}{n!} \left[\frac{1}{\gamma} \int_0^\infty d\omega \alpha(\omega) A_P^{\text{in}\dagger}(\omega) \right]^n |0\rangle, \end{aligned} \quad (5.8)$$

where $A_P^{\text{in}\dagger}$ is a creation operator for the incoming pump quanta. The expectation value for Q_P^{in} is then

$$\begin{aligned} \bar{Q}_P^{\text{in}}(t) \equiv \langle G, \gamma, \alpha | Q_P^{\text{in}}(t) | G, \gamma, \alpha \rangle \\ = -\frac{1}{2\gamma} \left[\frac{\hbar}{\pi R_P} \right]^{1/2} \int_0^\infty d\omega \omega^{-1/2} [\alpha(\omega) e^{-i\omega t} \\ + \text{c.c.}]. \end{aligned} \quad (5.9)$$

This is recognized as a Fourier expansion of a classical signal. One also readily sees that $\gamma \bar{Q}_P^{\text{in}}(t)$ is independent of γ . The fluctuation of Q_P^{in} about its mean is

$$(\Delta Q_P^{\text{in}})^2 = \frac{1}{R_P} \int_B \frac{d\omega}{2\pi} \frac{\hbar \omega}{2}. \quad (5.10)$$

In the limit $\gamma \rightarrow 0$ (5.7b) reduces to

$$Q_P(\omega_P) = 2Q_P^{\text{in}}(\omega_P). \quad (5.11)$$

In the limit $\gamma \rightarrow 0$, $Q_P(\omega_P)$ appearing in (5.7a) can be regarded as a classical variable since the quantum corrections, being of order $\gamma \Delta Q_P^{\text{in}}$, vanish. If the pump oscillator is very stable, producing a spectrally pure signal, $\alpha(\omega)$ will be very sharply peaked about ω_P^0 . Hence $Q_P(\omega_P)$ will have the form $Q_P \delta(\omega_P^0 - \omega_P)$ and Eq. (5.7a) reduces to

$$-i\omega_S R_S Q_S(\omega_S) + 2\gamma Q_P Q_S^\dagger(\omega_P^0 - \omega_S) = -i2\omega_S R_S Q_S^{\text{in}}(\omega_S). \quad (5.12)$$

From this equation and its Hermitian conjugate one can show (from now on we will write ω_P^0 as ω_P)

$$Q_S^{\text{out}}(\omega) = A Q_S^{\text{in}}(\omega) - i(A^2 - 1)^{1/2} e^{-i\phi_P} Q_S^{\text{in}\dagger}(\omega_P - \omega), \quad (5.13)$$

where ϕ_P is the phase of the pump signal defined by

$$Q_P = |Q_P| e^{-i\phi_P} \quad (5.14)$$

and A is the amplitude gain

$$A = \left| \frac{1 + \frac{4\gamma^2 |Q_P|^2}{\omega(\omega_P - \omega) R_S^2}}{1 - \frac{4\gamma^2 |Q_P|^2}{\omega(\omega_P - \omega) R_S^2}} \right|. \quad (5.15)$$

By choosing $4\gamma^2 |Q_P|^2 / [\omega(\omega_P - \omega) R_S^2]$ to be sufficiently close to 1, the gain can be made as large as desired. Choosing the pump phase such that $e^{-i\phi_P} = i$, Eq. (5.13) in terms of creation and annihilation operators becomes

$$A_S^{\text{out}}(\omega) = A A_S^{\text{in}}(\omega) + (A^2 - 1)^{1/2} A_S^{\text{in}\dagger}(\omega_P - \omega). \quad (5.16)$$

This transformation can be undone by a second DPA whose pump phase is chosen such that $e^{-i\phi_P} = -i$. Hence the transformation a DPA performs on a signal is noiseless and reversible.

In order to understand what the transformation (5.16) does to a signal it is convenient to write the incoming signal in component form as was done in (3.15)

$$V_{\text{in}}(t) = V'_{\text{in}}(t) \cos(\frac{1}{2}\omega_P t) + V''_{\text{in}}(t) \sin(\frac{1}{2}\omega_P t). \quad (5.17)$$

The outgoing signal operator then can be written as

$$V_{\text{out}}(t) = -(2A)^{-1} V'_{\text{in}}(t) \cos(\frac{1}{2}\omega_P t) - 2A V''_{\text{in}}(t) \sin(\frac{1}{2}\omega_P t) \quad (5.18)$$

provided the bandwidth B in (3.16) is restricted to

$$B < \frac{\omega_P}{2A^2}. \quad (5.19)$$

Hence the DPA is a phase sensitive amplifier having a gain of the form (5.2) such that $A_1 A_2 = 1$.

If the incoming signal consists only of vacuum fluctuations, then

$$\langle 0 | V_{\text{in}}'^2 | 0 \rangle = \langle 0 | V_{\text{in}}''^2 | 0 \rangle = R \int_B \frac{d\omega}{2\pi} \frac{\hbar\omega}{2}. \quad (5.20)$$

The $\cos(\frac{1}{2}\omega_P t)$ component of V_{out} then has fluctuations of the magnitude

$$(2A)^{-2} \langle 0 | V_{\text{in}}'^2 | 0 \rangle,$$

whereas the $\sin(\frac{1}{2}\omega_P t)$ component has fluctuations of the magnitude $(2A)^2 \langle 0 | V_{\text{in}}''^2 | 0 \rangle$. Hence the quantum noise fed into the input of the DPA comes out squeezed, having reduced quantum fluctuations in one component of the signal. This outgoing signal is referred to as squeezed noise^{1,2,23,24} in the gravitational physics literature and as a two-photon coherent state signal in the quantum optics literature.^{25,26}

Having analyzed the DPA, the linear phase insensitive parametric amplifier will now be discussed in order to comment on the ultimate noise performance of such a device. A realization of nondegenerate parametric amplifier is depicted in Fig. 1(a). The equivalent conservative circuit is shown in Fig. 1(b). The operation of this device in the negative resistance reflection mode will now be considered. In this mode the signal propagates towards the amplifier along transmission line R_S , the reflected and amplified signal will propagate back out along R_S . These two signals can be separated using a circulator as was done for the degenerate case in Fig. 3(a). For the proper operation of this device, the pump frequency f_P must be at the sum of the signal and idler frequencies, f_S and f_I , respectively,²²

$$f_P = f_S + f_I. \quad (5.21)$$

The circuit of Fig. 1(b) is straightforward to analyze, being only slightly more complicated than the DPA. Hence only the results of such a calculation will be quoted. The outgoing signal annihilation operator $A_S^{\text{out}}(\omega)$ expressed in terms of the incoming signal annihilation operator $A_S^{\text{in}}(\omega)$ and the incoming idler noise creation operator $A_I^{\text{in}\dagger}(\omega)$ is

$$A_S^{\text{out}}(\omega) = G^{1/2} A_S^{\text{in}}(\omega) - i(G - 1)^{1/2} A_I^{\text{in}\dagger}(\omega_P - \omega), \quad (5.22)$$

where G is the power gain given by

$$G = \left[\frac{1 + \frac{4\gamma^2 |Q_P|^2}{\omega_S \omega_I R_S R_I}}{1 - \frac{4\gamma^2 |Q_P|^2}{\omega_S \omega_I R_S R_I}} \right]^2 \quad (5.23)$$

which can be made large by choosing the pump amplitude such that

$$\frac{4\gamma^2 |Q_P|^2}{\omega_S \omega_I R_S R_I} \approx 1. \quad (5.24)$$

From (5.19), (2.1), and (2.9) one readily can show

$$I_S^{out}(t) = G^{1/2} I_S^{in}(t) - (G - 1)^{1/2} \frac{1}{2} \left[\frac{\hbar}{\pi R_S} \right]^{1/2} \int_B d\omega \omega^{1/2} [A_I^{in\dagger}(\omega_P - \omega) e^{-i\omega t} + \text{H.c.}] . \tag{5.25}$$

It is immediately evident that the incoming current is amplified by a factor of $G^{1/2}$. The second term on the right-hand side represents the noise coming from the idler resistor. If the idler resistor is cooled to a low enough temperature so that only vacuum fluctuations are coming from it, then this noise term contributes a noise power of

$$(G - 1) \int_B \frac{d\omega}{2\pi} \frac{\hbar\omega}{2}$$

to the amplified signal. In the limit of large gain this gives the often quoted noise power, referred to the input of the amplifier, of $\frac{1}{2} \hbar\omega$ per unit bandwidth.

The termination at the idler port is not required to put out noise distributed randomly over all phases. The termination could put out squeezed noise. Figure 4 depicts how this can be done: The termination consists of a resistor followed by a DPA, and therefore, the noise coming from the idler resistor is squeezed before being delivered to the idler tank circuit. The DPA is pumped at twice the center frequency of the idler tank circuit. Substituting an expression of the form (5.16) for A_I^{in} of Eq. (5.22), one readily can show for a sufficiently narrow bandwidth [see Eq. (5.19)] and for an idler resistor emitting vacuum fluctuations that

$$(\Delta I_S^{out})^2 = G(\Delta I_S^{in})^2 + (G - 1)(2A)^2 \cos^2(\omega_S^0 t) \int_B \frac{d\omega}{2\pi} \frac{\hbar\omega}{2} + (G - 1)(2A)^{-2} \sin^2(\omega_S^0 t) \int_0 \frac{d\omega}{2\pi} \frac{\hbar\omega}{2} , \tag{5.26}$$

where ω_S^0 is the center frequency of the signal tank circuit. Hence the noise is phase sensitive, and for the $\sin(\omega_S^0 t)$ component of the signal the amplifier noise power per unit bandwidth is reduced by a factor of $(2A)^{-2}$ over the standard result of $\frac{1}{2} \hbar\omega$. A phase insensitive linear amplifier can indeed keep one component of the amplified signal clean provided it is constructed properly.

Before moving on to back-action-evasion amplifiers, amplifiers with feedback networks will be briefly discussed. The amplifiers so far discussed work best when they are impedance matched to the signal source, that is, when they swallow up all the available power from the signal source. For certain types of measurements one would prefer that the measuring device not absorb any power from the circuit being measured. The ideal volt meter would absorb zero power from the circuit under test. Figure 5(a) shows a circuit suitable as the front end of a volt meter. It presents a high input impedance at its input port and, therefore, would absorb little power from the circuit under test. This circuit will be used as an op-

portunity to introduce a few techniques that will allow one to avoid going through the canonical quantization procedure of Sec. III each time one analyzes a different circuit. The main observation is that Kirchhoff's current and voltage laws give the correct Heisenberg equations of motion provided one includes the appropriate quantum noise term with each resistor. With the use of the definitions of Sec. II, Fig. 6 shows the Thévenin and Norton equivalents for a transmission line extending to infinity on the right or on the left in terms of the current operators

$$I_L = \frac{\partial Q_L}{\partial t} , \tag{5.27}$$

$$I_R = \frac{\partial Q_R}{\partial t} ,$$

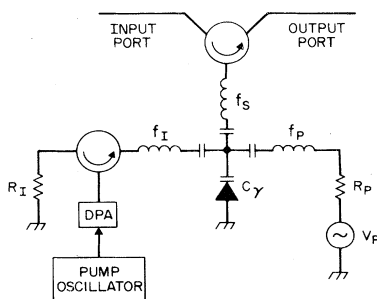


FIG. 4. A method of producing a linear amplifier that will have reduced noise fluctuations in one signal component. This is accomplished by squeezing the noise coming from the idler resistor using a DPA.

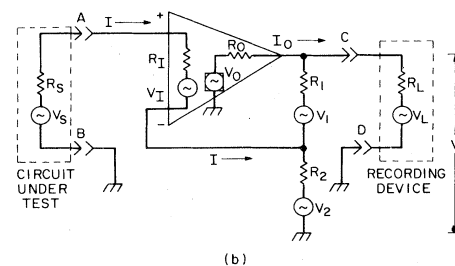
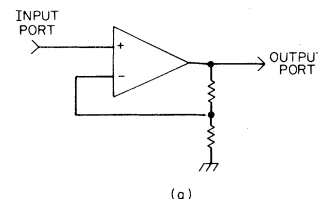


FIG. 5. (a) A voltage to voltage amplifier, suitable for the front end of a voltmeter. The circuit presents a high input impedance to the input port. (b) The same circuit with all noise and signal sources included.

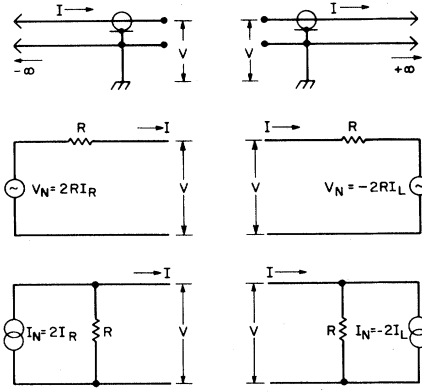


FIG. 6. Below each transmission line are shown successively the Thévenin and Norton equivalent circuits. Arrows indicate direction of positive current flow. I and V are defined by Eqs. (2.1) and (2.2). I_R and I_L are defined by Eq. (5.24).

where Q_I and Q_R are defined by Eq. (2.9). These equivalents are used in Fig. 5(b). An amplifier with differential inputs can be constructed from the linear phase insensitive parametric amplifier discussed earlier simply by transformer coupling to the input. The equivalent circuit for the amplifier is depicted in Fig. 5(b). The voltage generator V_O in the output port has been drawn inside a square to distinguish it from the other voltage generators. It is given by

$$V_O = 2R_O A (I - I_O) + 2R_O \left[A^2 - \frac{R_I}{R_O} \right]^{1/2} I_N, \quad (5.28)$$

where A is the amplitude gain and I_N is phase-conjugated noise generated inside the amplifier:

$$I_N = \frac{1}{2} \left[\frac{\hbar}{\pi R_I} \right]^{1/2} \int_0^\infty d\omega \omega^{1/2} [-iA_N^\dagger(\omega)e^{-i\omega t} + \text{H.c.}]. \quad (5.29)$$

I_O is the noise current at the input of the amplifier:

$$I_O = \frac{1}{2} \left[\frac{\hbar}{\pi R_O} \right]^{1/2} \int_0^\infty d\omega \omega^{1/2} [-iA_O(\omega)e^{-i\omega t} + \text{H.c.}]. \quad (5.30)$$

Note $V_O = -2RI_O$. Looking at (5.29) and (5.30), one sees that in I_N the creation and annihilation operators reverse roles when compared with the noise coming out of a conventional resistor. The phase conjugated noise arises from the fact that the relation between the quanta at the input and output of the amplifier²⁷ must be of the form (5.22). The distinction between the ordinary resistor noise and the phase-conjugated noise of an amplifier becomes important when considering the photon statistics as measured by a photodetector, the phase conjugation gives rise to spontaneous emission noise. With the currents and voltages labeled as in Fig. 5(b), Kirchoff's circuit laws give

$$\begin{aligned} 0 &= V_S - V_I - V_2 - (R_S + R_O + R_2)I - R_2(I_O - I_L), \\ V &= (I_O - I_L)(R_1 + R_2) + IR_2 + V_1 + V_2, \\ V &= I_L R_L + V_L, \\ V &= V_O - I_O R_O. \end{aligned} \quad (5.31)$$

Equations (5.28) and (5.31) form a complete set of linear operator equations which can be solved in a straightforward way for unknowns, such as V and I , in terms of the signal operator V_S and the noise operators V_I , V_O , V_1 , V_2 , V_L , and I_N . In the limit $A \rightarrow \infty$ the resulting expressions greatly simplify, and in particular (5.28) reduces to

$$I = I_O - I_N. \quad (5.32)$$

Since the only currents flowing at the input arise from noise sources I_O and I_N inside the amplifier, to the circuit under test, the input port presents an infinite input impedance. From (5.28) and (5.30) one can demonstrate that noise with a total noise power of $\hbar\omega$ per unit bandwidth is injected by the amplifier into the circuit under test.

The voltage delivered to the load is

$$\begin{aligned} V &= \frac{R_1 + R_2}{R_2} V_S - \frac{R_1}{R_2} V_2 + V_1 \\ &\quad - \left[R_1 + \frac{R_1 + R_2}{R_2} (R_1 - R_S) \right] I_O \\ &\quad + \left[R_1 + \frac{R_1 + R_2}{R_2} (R_1 + R_S) \right] I_N. \end{aligned} \quad (5.33)$$

For vacuum fluctuations coming out of the noise sources one finds

$$\begin{aligned} (\Delta V)^2 &= 4 \left[\frac{R_1 + R_2}{R_2} \right]^2 (\Delta V_S)^2 + 4 \left[\frac{R_1 + R_2}{R_2} \right] R_1 R_S \int_B \frac{d\omega}{2\pi} \frac{\hbar\omega}{2R_S} \\ &\quad + 2 \left[\left[R_1 + \frac{R_1 + R_2}{R_2} R_S \right] \frac{R_S}{R_I} + \left[\frac{R_1 + R_2}{R_2} \right]^2 R_1 R_S \right] \int_B \frac{d\omega}{2\pi} \frac{\hbar\omega}{2R_S}. \end{aligned} \quad (5.34)$$

The signal-to-noise ratio can be optimized with respect to R_I by solving

$$\frac{d(\Delta V)^2}{dR_I} = 0 \quad (5.35)$$

for R_I . The result is

$$R_I = \frac{R_2}{R_1 + R_2} \left[R_1 + R_S \frac{R_1 + R_2}{R_2} \right]. \quad (5.36)$$

Hence under optimal impedance matching (5.34) reduces to

$$\begin{aligned} (\Delta V)^2 = & 4 \left[\frac{R_1 + R_2}{R_2} \right]^2 (\Delta V_S)^2 \\ & + 4 \left[\frac{R_1 + R_2}{2} \right]^2 R_S^2 \int_B \frac{d\omega}{2\pi} \frac{\hbar\omega}{2R_S} \\ & + 4 \frac{R_1 + R_2}{R_2} R_1 R_S \int_B \frac{d\omega}{2\pi} \frac{\hbar\omega}{2R_S}. \end{aligned} \quad (5.37)$$

The first two terms are what one would expect for an amplifier operating at the quantum limit ($\frac{1}{2}\hbar\omega$ noise power per unit bandwidth when referred to the input). The last term can be made negligible provided R_1 and R_2 are chosen such that

$$R_S \gg \frac{R_1 R_2}{R_1 + R_2}. \quad (5.38)$$

To conclude, an ideal voltmeter, whose internal noise sources eject noise uniformly over all phases, must inject noise into the system being measured with a noise power of $1\hbar\omega$ per unit bandwidth. Under optimal impedance matching conditions, the noise in the signal delivered by the amplifier to the display device has a noise power per unit bandwidth of $\frac{1}{2}\hbar\omega$.

It is hoped that this exercise has convinced the reader that a full quantum analysis of the optimal performance of even relatively complicated electronic circuits may be done in a straightforward manner. In the next section it is shown how the noise limitations of an ideal voltmeter can be overcome with phase sensitive detection schemes.

VI. BACK-ACTION-EVADING MEASUREMENT

In the last section it was pointed out that there are two fundamental limitations which quantum mechanics places on an ideal voltmeter whose internal noise sources emit noise uniformly over all phases. In particular the voltmeter must inject noise with a noise power of $1\hbar\omega$ per unit bandwidth into the circuit whose voltage is being measured. This is called back-action noise. Further, the amplified signal which the voltmeter ultimately uses to drive a display device has a noise power of $\frac{1}{2}\hbar\omega$ per unit bandwidth when referred to the voltmeter's input. In this section a few detection schemes are presented which are able to overcome these limitations, at least for one component of the signal being measured. These measuring schemes have been dubbed as back-action evasion by Caves.¹ A number of back-action-evading detection schemes have

been proposed in the literature.² The three which will be discussed here are shown in Figs. 7(a)–7(c). These back-action-evading detection schemes are able to achieve good signal-to-noise ratios even when the system under test is poorly impedance matched to the detector. Hence in Figs. 7(a) and 7(b) an impedance mismatch K has been inserted between the system under test and the input port of the measuring device.

The operation of the circuit in Fig. 7(a) will now be discussed.²⁸ A similar device was described by Shapiro.²⁹ The terminating resistor R_T is emitting equilibrium noise which is directed towards DPA1. The voltage of this noise, appearing at node 1 is, when written in component form relative to ω_0 , half the pump frequency,

$$V_1 = V'_N \cos(\omega_0 t) + V''_N \sin(\omega_0 t). \quad (6.1)$$

The voltage of the signal delivered by DPA1 to node 2 is then, by choosing the pump oscillator phase properly,

$$V_2 = G^{-1} V'_N \cos(\omega_0 t) + G V''_N \sin(\omega_0 t), \quad (6.2)$$

where G is the gain of DPA1. Let the voltage, at node 4, of the signal propagating from the system under test to the impedance mismatch be written as

$$V_S^{\text{in}} = V'_S \cos(\omega_0 t) + V''_S \sin(\omega_0 t). \quad (6.3)$$

A fraction K of this signal makes it past the impedance mismatch. On the other hand, a fraction $(1-K^2)^{1/2}$ of V_2 is reflected off the impedance mismatch. Hence the signal appearing at node 5 is

$$\begin{aligned} V_5 = & K V'_S \cos(\omega_0 t) + K V''_S \sin(\omega_0 t) \\ & + (1-K^2)^{1/2} [G^{-1} V'_N \cos(\omega_0 t) + G V''_N \sin(\omega_0 t)]. \end{aligned} \quad (6.4)$$

DPA2 is adjusted via the phase shifter to amplify in quadrature to DPA1. Choosing DPA1 and DPA2 to have the same gain, the voltage of the signal delivered to the output port, node 6, is

$$\begin{aligned} V_O = & G K V'_S \cos(\omega_0 t) + G^{-1} K V''_S \sin(\omega_0 t) \\ & + (1-K^2)^{1/2} [V'_N \cos(\omega_0 t) + V''_N \sin(\omega_0 t)]. \end{aligned} \quad (6.5)$$

The signal-to-noise ratio for V_S is then

$$\frac{S}{N} = \frac{G^2 K^2 \langle V_S'^2 \rangle}{(1-K^2) \langle V_N'^2 \rangle}. \quad (6.6)$$

In the limit $G \rightarrow \infty$, the signal-to-noise ratio becomes arbitrarily good. The voltage V_S^{out} of the signal propagating from the impedance mismatch back toward the system under test is

$$\begin{aligned} V_S^{\text{out}} = & (1-K^2)^{1/2} [V'_S \cos(\omega_0 t) + V''_S \sin(\omega_0 t)] \\ = & K G^{-1} V'_N \cos(\omega_0 t) + K G V''_N \sin(\omega_0 t). \end{aligned} \quad (6.7)$$

One can see that in the limit $K \rightarrow 0$, $G \rightarrow \infty$ such that $K G \rightarrow \infty$ the signal-to-noise ratio (6.6) becomes arbitrarily good and the fraction of the signal V_S^{in} absorbed by the measuring device becomes arbitrarily small. Further, the $\cos(\omega_0 t)$ component of V_S^{out} is uncontaminated with back-action noise in this limit.

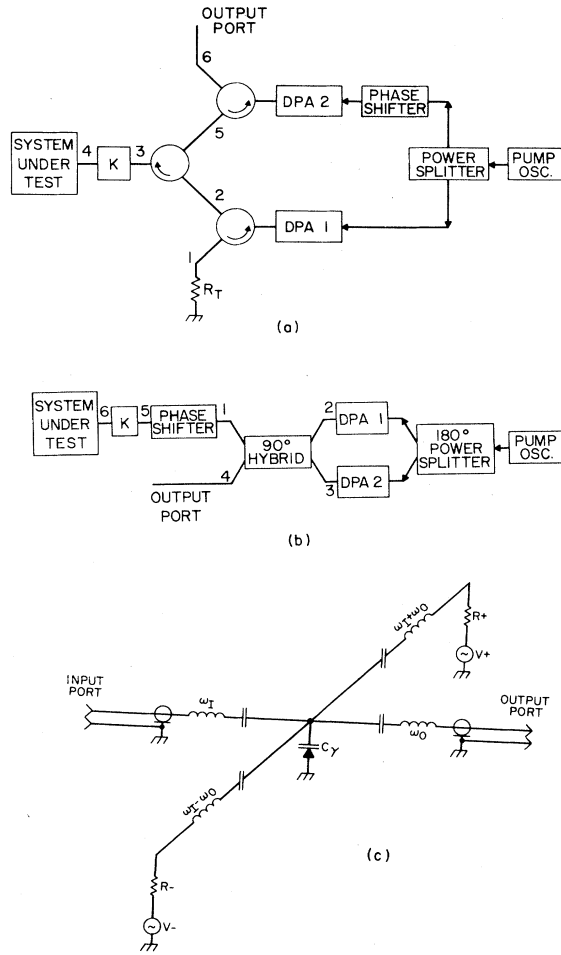


FIG. 7. Three embodiments of back-action-evasion amplifiers.

The circuit just discussed requires circulators to direct the signal flow through the circuit. Figure 7(b) shows how two DPA's, pumped in quadrature, can be combined in a balanced configuration to accomplish back-action evasion. Furthermore, since 3-dB 90° hybrid couplers can be constructed out of lumped circuit components,³⁰ this circuit more readily can be realized at the low frequencies where Weber bar gravitational wave antennas operate. A lumped circuit realization of a 3-dB 90° hybrid coupler is depicted in Fig. 8. This device is narrow band and correct operating performance is obtained provided

$$\begin{aligned} 1 &= \omega^2 L (C_0 + C_1), \\ 1 &= \omega^2 C_0 (C_0 + 2C_1) Z^2, \\ 1 &= \omega C_1 Z, \end{aligned} \quad (6.8)$$

where Z is the transmission line impedance. The ports of Fig. 8 and the nodes of Fig. 7(b) have been labeled to make the numbering between the two correspond. Let $Q_1^{\text{in}}, Q_2^{\text{in}}, Q_3^{\text{in}}, Q_4^{\text{in}}$ denote the charges of the signals, with time dependence $e^{-i\omega t}$, entering, respectively, ports 1–4 of the 90° hybrid. Similarly $Q_1^{\text{out}}, Q_2^{\text{out}}, Q_3^{\text{out}}, Q_4^{\text{out}}$ denote

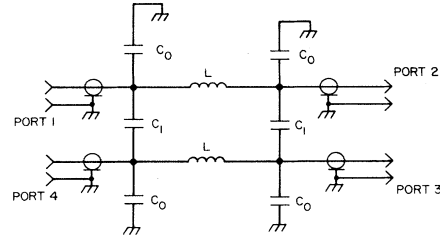


FIG. 8. A lumped circuit realization of a 3-dB 90° hybrid coupler.

the signals leaving the 90° hybrid. Introducing the column vectors

$$\vec{Q}^{\text{in}} = \begin{bmatrix} Q_1^{\text{in}} \\ Q_2^{\text{in}} \\ Q_3^{\text{in}} \\ Q_4^{\text{in}} \end{bmatrix}, \quad \vec{Q}^{\text{out}} = \begin{bmatrix} Q_1^{\text{out}} \\ Q_2^{\text{out}} \\ Q_3^{\text{out}} \\ Q_4^{\text{out}} \end{bmatrix}, \quad (6.9)$$

the scattering matrix \underline{S}

$$\vec{Q}^{\text{out}} = \underline{S} \vec{Q}^{\text{in}}, \quad (6.10)$$

has the form

$$\underline{S} = \frac{e^{i\phi}}{\sqrt{2}} \begin{bmatrix} 0 & 1 & -i & 0 \\ 1 & 0 & 0 & -i \\ -i & 0 & 0 & 1 \\ 0 & -i & 1 & 0 \end{bmatrix}, \quad (6.11)$$

where $\phi = -\pi/4$ is the overall phase shift of the 90° hybrid.

The balanced DPA operates as follows: Let V_1^{in} and V_4^{in} denote the voltage of the signals propagating into the 90° hybrid coupler from nodes 1 and 4, respectively. In component form

$$\begin{aligned} V_1^{\text{in}} &= V_1^{\text{in}'} \cos(\omega_0 t) + V_1^{\text{in}''} \sin(\omega_0 t), \\ V_4^{\text{in}} &= V_4^{\text{in}'} \cos(\omega_0 t) + V_4^{\text{in}''} \sin(\omega_0 t). \end{aligned} \quad (6.12)$$

Let V_1^{out} and V_4^{out} denote the voltage of the signals propagating out of the 90° hybrid coupler at nodes 1 and 4, respectively. One then has

$$\begin{aligned} V_4^{\text{out}} &= G^{-1} V_1^{\text{in}'} \cos(\omega_0 t + \phi) + G V_1^{\text{in}''} \sin(\omega_0 t + \phi), \\ V_1^{\text{out}} &= G V_4^{\text{in}'} \cos(\omega_0 t + \phi) + G^{-1} V_4^{\text{in}''} \sin(\omega_0 t + \phi). \end{aligned} \quad (6.13)$$

Consider now the signal V_S^{in} propagating from the system under test towards the impedance mismatch which we will decompose into quadrature form as follows:

$$V_S^{\text{in}} = V_S^{\text{in}'} \cos(\omega_0 t - \theta) + V_S^{\text{in}''} \sin(\omega_0 t - \theta), \quad (6.14)$$

where θ is the phase shift produced by the phase shifter. A fraction K of this signal makes it past the impedance mismatch, and a fraction $(1-K^2)^{1/2}$ of the noise V_1^{out} is, after passing through the phase shifter, reflected back. Hence the voltage V_5^{in} of the signal at node 5, propagating from the mismatch to the phase shifter, is

$$V_S^{\text{in}} = K[V_S^{\text{in}'} \cos(\omega_O t - \theta) + V_S^{\text{in}''} \sin(\omega_O t - \theta)] + (1 - K^2)^{1/2}[G V_4^{\text{in}'} \cos(\omega_O t + \phi + \theta) + G^{-1} V_4^{\text{in}''} \sin(\omega_O t + \phi + \theta)]. \quad (6.15)$$

Passing through the phase shifter

$$V_I^{\text{in}} = K[V_S^{\text{in}'} \cos(\omega_O t) + V_S^{\text{in}''} \sin(\omega_O t)] + (1 - K^2)^{1/2}[G V_4^{\text{in}'} \cos(\omega_O t + \phi + 2\theta) + G^{-1} V_4^{\text{in}''} \sin(\omega_O t + \phi + 2\theta)]. \quad (6.16)$$

If the phase shifter is set such that $\phi + 2\theta = 0$, one has

$$V_4^{\text{out}} = G^{-1} K V_S^{\text{in}'} \cos(\omega_O t + \phi) + G K V_S^{\text{in}''} \sin(\omega_O t + \phi) + (1 - K^2)^{1/2}[V_4^{\text{in}'} \cos(\omega_O t + \phi) + V_4^{\text{in}''} \sin(\omega_O t + \phi)]. \quad (6.17)$$

For the signal propagating from the impedance mismatch K to the system under test, one has

$$V_S^{\text{out}} = (1 - K)^{1/2}[V_S^{\text{in}'} \cos(\omega_O t - \theta) + V_S^{\text{in}''} \sin(\omega_O t - \theta)] + K[G V_4^{\text{in}'} \cos(\omega_O t - \theta) + G^{-1} V_4^{\text{in}''} \sin(\omega_O t - \theta)]. \quad (6.18)$$

From (6.17) and (6.18), analogous to the discussion surrounding (6.5) and (6.7), one sees that this device, in the limit $KG \rightarrow \infty$ with $K \rightarrow 0$, measures $V_S^{\text{in}''}$ with arbitrarily good signal-to-noise ratio, absorbs negligible amount of the signal's power, and does not dump noise into the component of the signal that is being measured.

As a final example of a back-action-evading measuring device, consider the circuit shown in Fig. 7(c). This four-wave mixer is closely related to a scheme Bocko and Johnson are developing³¹ to perform back-action evasion on a mechanical oscillator. The signal entering the input port of the circuit of Fig. 7 oscillates at ω_I and the signal leaving the output port oscillates at ω_O . Because of the symmetry of the circuit, it is clear that the input and output ports can be interchanged. The circuit has two pump oscillators: One, V_+ , oscillates with a time dependence $\cos(\omega_I + \omega_O)t$, and the other, V_- , has the same amplitude and oscillates with a time dependence $\cos(\omega_I - \omega_O)t$. The nonlinear mixing in C_γ then produces an effective time-dependent capacitance whose voltage-charge relationship is

$$V = \left[\frac{1}{C_\gamma} + \gamma Q_P \cos(\omega_I t) \cos(\omega_O t) \right] Q, \quad (6.19)$$

where Q_P is a constant. Isolation between the various branches of the circuit is accomplished with tank circuits of sufficiently high quality factor. As an alternative, one could go to balanced or double balanced configurations to isolate the pumps from the signal branches of the circuit. A balanced configuration, taking advantage of additional decoupling that can be achieved in an electromechanical system, is employed by Bocko and Johnson.³¹ The circuit of Fig. 7(c) is again very straightforward to analyze fully quantum mechanically. Hence only the results will be displayed here. Let V_I^{in} be the voltage of the signal entering the input port and V_O^{in} be the voltage of the back-action noise entering the output port from external electronics. Similarly, V_I^{out} and V_O^{out} denote the voltages of the signals leaving the input and output ports, respectively. Writing the incoming signals in component form,

$$\begin{aligned} V_O^{\text{in}} &= V_O^{\text{in}'} \cos(\omega_O t) + V_O^{\text{in}''} \sin(\omega_O t), \\ V_I^{\text{in}} &= V_I^{\text{in}'} \cos(\omega_I t) + V_I^{\text{in}''} \sin(\omega_I t), \end{aligned} \quad (6.20)$$

the outgoing signals are given by

$$V_O^{\text{out}} = -V_O^{\text{in}} - \frac{\gamma Q_P}{\omega_I R_I} V_I^{\text{in}''} \cos(\omega_O t), \quad (6.21a)$$

$$V_I^{\text{out}} = -V_I^{\text{in}} - \frac{\gamma Q_P}{\omega_O R_O} V_O^{\text{in}''} \cos(\omega_I t). \quad (6.21b)$$

Since V_O^{in} and V_I^{in} change sign after being reflected off their respective ports, it is clear that the input and output ports present zero impedance, i.e., a short circuit, to the external world. If $\gamma Q_P / (\omega_I R_I)$ becomes large, then V_O^{out} reports the value of $V_I^{\text{in}''}$, the $\sin(\omega_I t)$ component of the incoming signal. The back-action noise, as can be seen from (6.21b), is dumped into the $\cos(\omega_I t)$ component of the signal at the input port. Because of its low input impedance, the device of Fig. 7(c) is most appropriate for phase-sensitive back-action-evading current measurements. Four-wave mixers can also be constructed with high input impedance. Alternatively, a quarter-wave section of transmission line could be used to transform a low impedance into a high impedance.

Before leaving this section, it is worth pointing out that the back-action measuring devices discussed here approximate a von Neumann measuring device³² in that the system being measured is forced into an eigenstate of the operator whose eigenvalue is being measured. To illustrate this, consider Fig. 9 where two back-action-evading devices, BAE1 and BAE2, successively monitor the signal

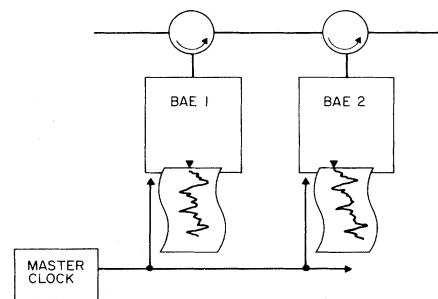


FIG. 9. Two back-action-evading measuring devices, BAE1 and BAE2, controlled by the same master clock. If BAE1 and BAE2 are adjusted to monitor the same signal component, their chart recorder outputs will be highly correlated. The back-action-evading measuring process approximates a von Neumann measuring process in which the system being measured is forced into an eigenstate of the operator whose eigenvalue is being measured.

propagating along a transmission line. Both BAE's are phase locked to the same master clock so that they monitor the same component, say the V'_S component of the signal V_S propagating to the right along the transmission line. Let V_1 and V_2 denote, respectively, the operator for the output of BAE1 and BAE2. From (6.5) and (6.7) one then has

$$\begin{aligned} V_1 &= GK V'_S \cos(\omega_0 t) + G^{-1} K V''_S \sin(\omega_0 t) \\ &\quad + (1-K^2)^{1/2} V_{N1}, \\ V_2 &= GK (1-K^2)^{1/2} V'_S \cos(\omega_0 t) \\ &\quad + GK^{-1} (1-K^2)^{1/2} V''_S \sin(\omega_0 t) \\ &\quad + K^2 V_{N1} + (1-K^2)^{1/2} V_{N2}, \end{aligned} \quad (6.22)$$

where V_{N1} and V_{N2} are the noise operators for the noise generated in BAE1 and BAE2, respectively. In the limit $K \rightarrow 0$, holding GK fixed, one obtains

$$\begin{aligned} V_1 &= GK V'_S \cos(\omega_0 t) + V_{N1}, \\ V_2 &= GK V'_S \cos(\omega_0 t) + V_{N2}. \end{aligned} \quad (6.23)$$

Now since V_{N1} and V_{N2} , being equilibrium noise coming out of a resistor, are independent of G and K , V_1 and V_2 become as good a reproduction of V'_S as desired provided GK is chosen to be sufficiently large. Hence V_1 and V_2 report the same eigenvalue for V'_S , as can be demonstrated by working out the correlation coefficient between V_1 and V_2

$$\begin{aligned} r &\equiv \frac{\langle V_1 V_2 \rangle - \langle V_1 \rangle \langle V_2 \rangle}{[\langle V_1^2 \rangle - \langle V_1 \rangle^2] [\langle V_2^2 \rangle - \langle V_2 \rangle^2]^{1/2}} \\ &\approx 1 - \frac{\langle V_N^2 \rangle}{G^2 K^2 (\langle V_S'^2 \rangle - \langle V_S' \rangle^2)}, \end{aligned} \quad (6.24)$$

where the last line has been obtained by assuming $\langle V_{N1} \rangle = \langle V_{N2} \rangle = 0$ and $\langle V_{N1}^2 \rangle = \langle V_{N2}^2 \rangle = \langle V_N^2 \rangle$. Hence in the limit $GK \rightarrow \infty$, the two chart recorder traces become completely correlated.

VII. JOSEPHSON JUNCTIONS

A number of parametric amplifiers and four-wave mixer circuits have been discussed in the last few sections. In these circuits, nonlinear capacitors were used to do the reactive mixing to produce power amplification. At the low temperatures necessary to reduce thermal fluctuations, the nonlinear inductance provided by the Josephson junction is more suitable for reactive mixing. In this section it is shown how the resistively-shunted-junction (RSJ) model of a Josephson junction can be handled readily within the framework of the techniques presented earlier in this paper. In particular, a Lagrangian density for a Josephson junction is written down which generates Heisenberg equations of motion appropriate for the RSJ model. These equations of motion will be nonlinear and no attempt will be made to solve them here. However, the Heisenberg equations of motion do provide a starting point for perturbation calculations of the behavior of electronic circuits incorporating Josephson junctions. Such an

approach was used by Koch, Van Harlingen, and Clark.⁶ Alternatively, as was done by Caldeira and Leggett,⁵ Feynman path-integral techniques³³ may be applied to the Lagrangian density to obtain the quantum behavior of electronic circuits when the nonlinearities are too strong to be handled by perturbation techniques. We will use this section as an opportunity to show how a certain class of nonlinear resistances may be treated in a Lagrangian formalism. In particular, let x be some generalized position coordinate and X be a heat bath coordinate, then, as Caldeira and Leggett have shown,³⁴ a term in the Lagrangian of the form

$$f(x) \frac{dX}{dt}$$

gives rise to x -dependent damping of the form

$$\left| \frac{\partial f(x)}{\partial x} \right|^2 \frac{dx}{dt}.$$

The $\cos\phi$ dissipative term in the Josephson current relationship³⁵ belongs to this class of nonlinear resistances.

The circuit to be considered is depicted in Fig. 10. It consists of a dissipative Josephson junction shunting a transmission line which runs off to some electronic instrumentation. The Lagrangian density describing this circuit is

$$\mathcal{L} = \delta(x) \frac{\hbar}{2e} \left[I_J \cos\phi + \phi \frac{\partial Q}{\partial t} - \phi \frac{\partial Q_R}{\partial t} - 2\xi \sin \left[\frac{\phi}{2} \right] \frac{\partial Q_c}{\partial t} \right] \quad (7.1a)$$

$$+ H_-(x) \left[\frac{L_T}{2} \left[\frac{\partial Q}{\partial t} \right]^2 - \frac{1}{2C_T} \left[\frac{\partial Q}{\partial x} \right]^2 \right] \quad (7.1b)$$

$$+ H_+(x) \left[\frac{L_T^R}{2} \left[\frac{\partial Q_R}{\partial t} \right]^2 - \frac{1}{2C_T^R} \left[\frac{\partial Q_R}{\partial x} \right]^2 \right] \quad (7.1c)$$

$$+ H_+(x) \left[\frac{L_T^c}{2} \left[\frac{\partial Q_c}{\partial t} \right]^2 - \frac{1}{2C_T^c} \left[\frac{\partial Q_c}{\partial x} \right]^2 \right], \quad (7.1d)$$

where H_+ is the usual Heaviside function

$$H_+(x) = \begin{cases} 1, & x \geq 0 \\ 0, & \text{otherwise} \end{cases}$$

and

$$H_-(x) = \begin{cases} 0, & x \geq 0 \\ 1, & \text{otherwise} \end{cases}.$$

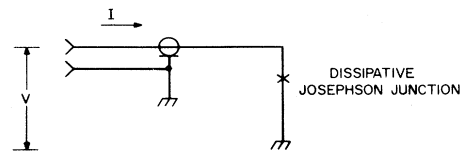


FIG. 10. A dissipative Josephson junction terminating a transmission line.

The terms labeled (7.1a), (7.1c), and (7.1d) belong to the junction itself. The term (7.1a) describes the reactive non-linearity and the coupling to the heat baths. Terms (7.1c) and (7.1d) are the heat baths associated with the dissipative terms of the junction. The transmission line attached to the junction is described by the term labeled (7.1b).

It easily is demonstrated that the Lagrangian density (7.1a)–(7.1d) generates the right equations of motion, and, therefore, provides an appropriate starting point for canonical quantization. The Euler-Lagrange equation for ϕ yields

$$I \equiv \frac{\partial Q}{\partial t} = I_J \sin \phi + \frac{\partial Q_R}{\partial t} + \xi \cos \left[\frac{\phi}{2} \right] \frac{dQ_c}{dt}. \quad (7.2)$$

The Euler-Lagrange equation for Q yields the Josephson frequency relation

$$\frac{d\phi}{dt} = \frac{2e}{\hbar} V, \quad (7.3)$$

where

$$V \equiv - \frac{1}{C_T} \frac{\partial Q}{\partial x} \Big|_{x=0^-}$$

is the voltage across the transmission line at $x=0$ and, hence, the voltage across the junction. The Euler-Lagrange equation for Q_R yields, upon using (7.3),

$$V = - \frac{1}{C_T^R} \frac{\partial Q_R}{\partial x} \Big|_{x=0^+}. \quad (7.4)$$

Similarly, the Euler-Lagrange equation for Q_c yields

$$\xi \cos \left[\frac{\phi}{2} \right] V = - \frac{1}{C_T^c} \frac{\partial Q_c}{\partial x} \Big|_{x=0^+}. \quad (7.5)$$

Using the same method by which (3.13) was derived, (7.4) and (7.5) can be put into the form

$$\frac{dQ_R}{dt} = \frac{V}{R} + \frac{dQ_R^{\text{in}}}{dt}, \quad (7.6)$$

$$\frac{dQ_c}{dt} = \xi \cos \left[\frac{\phi}{2} \right] \frac{V}{R_c} + 2 \frac{dQ_c^{\text{in}}}{dt}. \quad (7.7)$$

Substituting these expressions into (7.2) yields, remembering that $\cos^2(\phi/2) = \frac{1}{2}(1 + \cos \phi)$,

$$I = I_J \sin \phi + \frac{V}{R} + \frac{\xi^2}{2} (1 + \cos \phi) \frac{V}{R_c} + 2 \frac{dQ_R^{\text{in}}}{dt} + 2\xi \cos \left[\frac{\phi}{2} \right] \frac{dQ_c^{\text{in}}}{dt}. \quad (7.8)$$

This equation is recognized as the Josephson-junction current relationship with linear V/R dissipation and $\cos \phi$ dependent dissipation. The last two terms on the right-hand side of Eq. (7.8) are the fluctuation terms associated with the linear and $\cos \phi$ dependent dissipation. Equations

(7.2)–(7.8) are correct Heisenberg equations of motion (provided the operators are normal ordered¹⁴) and the fluctuation operators Q_R^{in} and Q_c^{in} are independent of each other and have the form given in Eq. (3.15). Hence it has been shown how the RSJ model of the Josephson junction can be quantized to recover the operator character of I , V , and ϕ .

The status and sign of the $\cos \phi$ dissipation is controversial^{36,37} with experimental evidence suggesting that it is negative. A $-\cos \phi$ dependent dissipation can be generated by replacing $\sin(\phi/2)$ with $\cos(\phi/2)$ in the Lagrangian density (7.1a).

VIII. TIME-DEPENDENT RESISTORS AND RESISTIVE MIXERS

In this section time-dependent resistors are treated by introducing a time-dependent coupling to a heat bath. The time-dependent resistor then can be used to calculate the ideal quantum performance of resistive mixers. As an example, the quantum performance of an ideal ring mixer will be discussed. It is pointed out that, for certain detection configurations, mixers in principle can be noiseless. Homodyne detection, a phase sensitive detection scheme in which the local oscillator frequency and signal carrier frequency are the same and a definite phase relationship between the signal and local oscillator is maintained, in principle can be noiseless. In the heterodyne detection process, where no special frequency relationship between the local oscillator and signal exists, one quadrature component of the incoming signal can still be processed noiselessly provided the mixer's image port is terminated with a squeezed-state source. These results were first recognized by Yuen and Shapiro³⁸ but deserve better publicity among the Josephson-junction community, particularly in light of the success that has already been achieved in operating superconductor-insulator-superconductor (SIS) junction mixers close to the standard quantum limit. It is hoped that the techniques presented here will be useful in designing SIS mixer configurations capable of operating below the standard quantum limit. Extensive theoretical work has been carried out by Tucker³⁹ on SIS mixers. This work is semiclassical in that the microscopic physics of the SIS junction is treated quantum mechanically while the electromagnetic field is treated classically. The approach presented here addresses the following question: Given the classical behavior of the device, what is the lowest noise performance that such a device in principle could realize quantum mechanically? In this approach the electromagnetic degrees of freedom (voltages and currents) are treated quantum mechanically and the microscopic physics is ignored. In general, one can expect the microscopic physics to introduce extra noise. Hence it would be desirable to have a full theory of SIS mixers in which both the microscopic physics and the electromagnetic fields are treated quantum mechanically.

As an illustration of how time-dependent resistors can be treated quantum mechanically, consider the Lagrangian density:

$$\begin{aligned} \mathcal{L} = & \delta(x) \left[f(t) \frac{dQ}{dt} Q_H - \frac{R_H}{f(t)} \frac{df(t)}{dt} \frac{Q_H^2}{2} \right] \\ & + H_+(x) \left[\frac{L_H^T}{2} \left[\frac{\partial Q_H}{\partial t} \right]^2 - \frac{1}{2C_H^T} \left[\frac{\partial Q_H}{\partial x} \right]^2 \right] \\ & + H_-(x) \left[\frac{L^T}{2} \left[\frac{\partial Q}{\partial t} \right]^2 - \frac{1}{2C^T} \left[\frac{\partial Q}{\partial x} \right]^2 \right]. \quad (8.1) \end{aligned}$$

Q represents the charge flowing along a transmission line which is terminated by a time-dependent resistor. Time-dependent dissipation is accomplished by coupling Q in a time-dependent manner to the heat bath field Q_H . $f(t)$ is the time varying coupling parameter and R_H is the impedance of the heat bath. From the equations of motion generated by (8.1) one readily can derive

$$V = \frac{|f(t)|^2}{R_H} I + 2f(t) \frac{dQ_H^{\text{in}}}{dt}, \quad (8.2)$$

where I is the current flowing through the nonlinear resistor and V is the voltage developed across the resistor. The fluctuations associated with the time-dependent dissipation $|f(t)|^2/R_H$ are given by $2f(t)dQ_H^{\text{in}}/dt$. Let dQ^{in}/dt denote the current of the signal propagating along the transmission line towards the nonlinear resistance. The current dQ^{out}/dt of the signal reflected off of the nonlinear resistance is

$$\frac{dQ^{\text{out}}}{dt} = \left| \frac{ZR_H - f^2(t)}{ZR_H + f^2(t)} \right| \frac{dQ^{\text{in}}}{dt} - \frac{2R_H f(t)}{ZR_H + f^2(t)} \frac{dQ_H^{\text{in}}}{dt}. \quad (8.3)$$

Having demonstrated how to treat time-dependent resistors quantum mechanically, the ring mixer will now be discussed. A practical embodiment of a ring mixer is depicted in Fig. 11(a). A pump oscillator oscillating at ω_p modulates the resistance of the diodes. An equivalent circuit consisting of time-dependent resistors $r(t)$ having a periodic time dependence with frequency ω_p is shown in Fig. 11(b). This and other mixer circuits can be analyzed quantum mechanically in a straightforward extension of the techniques of classical mixer theory.⁴⁰ A particularly

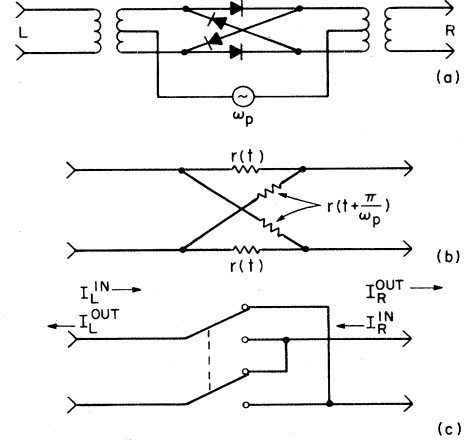


FIG. 11. (a) A practical realization of a ring mixer. (b) An equivalent electrical circuit constructed out of time-dependent resistors $r(t)$. (c) An equivalent circuit when $r(t)$ switches from zero to infinite resistance.

simple case occurs when $r(t)$ quickly switches between zero resistance and infinite resistance. In this limit the second term on the right-hand side of (8.3) vanishes. No noise from the resistor heat bath is injected into the circuit. Hence in this limit the ring mixer becomes equivalent to the dissipationless switching circuit of Fig. 11(c). The relation between the incoming and outgoing signals becomes

$$\begin{aligned} I_R^{\text{out}} &= \epsilon(t) I_R^{\text{in}}, \\ I_R^{\text{out}} &= \epsilon(t) I_L^{\text{in}}, \end{aligned} \quad (8.4)$$

where $\epsilon(t)$ is a periodic square wave switching between $+1$ and -1 . Taking $\epsilon(t)$ to be defined by

$$\epsilon(t) = \begin{cases} 1, & -\pi/2 < \omega_p t < \pi/2 \\ -1, & \pi/2 < \omega_p t < 3\pi/2 \end{cases} \quad (8.5)$$

one has upon Fourier expanding

$$\epsilon(t) = \frac{2}{\pi} \sum_{n=1,3,5,\dots} \frac{(-1)^{(n-1)/2}}{n} (e^{-in\omega_p t} + e^{in\omega_p t}). \quad (8.6)$$

So in particular

$$I_R^{\text{out}}(t) = \frac{2}{\pi} \sum_{n=1,3,5,\dots} \frac{(-1)^{(n-1)/2}}{n} \int_0^\infty d\omega [I_L^{\text{in}}(\omega) e^{-i(n\omega_p + \omega)t} + I_L^{\text{in}}(\omega) e^{i(n\omega_p - \omega)t} + \text{H.c.}]. \quad (8.7)$$

Consider the output at frequency ω_0 with $\omega_0 < \omega_p$, then in terms of annihilation operators

$$\sqrt{\omega_0} A_R^{\text{out}}(\omega_0) = \frac{2}{\pi} \sum_{n=1,3,5,\dots} \frac{(-1)^{n-1}}{n} [\sqrt{n\omega_p + \omega_0} A_L^{\text{in}}(n\omega_p + \omega_0) + \sqrt{n\omega_p - \omega_0} A_L^{\text{in}\dagger}(n\omega_p - \omega_0)]. \quad (8.8)$$

Similarly, the complete quantum-mechanical scattering matrix for the ring mixer can be obtained.

Optimum mixer performance is obtained by properly terminating and impedance matching the input and output ports of a resistive mixer. A mixer configuration hav-

ing power conversion of unity is shown in Fig. 12(a). The box with the X represents the ring mixer, and L and R denote the left-hand and right-hand ports, respectively. All signals at the left-hand port are short-circuited except for a band about the signal frequency ω_0 . All the signals

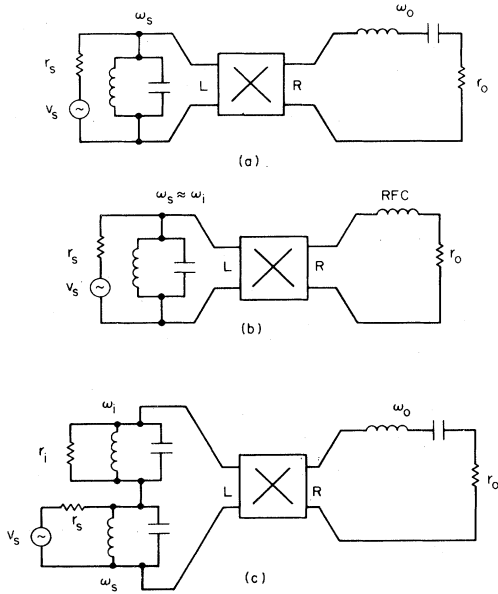


FIG. 12. Some resistive mixer configurations. (a) A frequency down converter where $\omega_0 = \omega_s - \omega_p$. (b) A homodyne detector where $\omega_s = \omega_p$ and the output is at dc. (c) A frequency converter with image frequency termination where $\omega_i = \omega_p - \omega_0$ and $\omega_s = \omega_p + \omega_0$.

at the right-hand port are open-circuited except for those lying in a band about ω_0 . Consider a down converter where ω_0 is small compared to the pump frequency ω_p and let the relation between the signal and output frequency be

$$\omega_s = \omega_p + \omega_0.$$

Then under optimal impedance matching,

$$\frac{r_s}{r_0} = \frac{\pi^2}{4}, \quad (8.9)$$

the relation between the incoming signal quanta A_s^{in} and the quanta A_0^{out} delivered to the load r_0 is

$$A_0^{\text{out}}(\omega_0) = \left[\frac{\omega_p}{\omega_0} + 1 \right]^{1/2} A_s^{\text{in}}(\omega_p + \omega_0) + \left[\frac{\omega_p}{\omega_0} \right]^{1/2} A_N^\dagger, \quad (8.10)$$

where A_N^\dagger is the annihilation operator for down converted noise at infinite frequency. This expression is similar to that of the linear amplifier (5.22). Hence when $\omega_s \gg \omega_0$, the noise added to the down converted signal is $\frac{1}{2}\hbar\omega$ per unit bandwidth when referred to the input. The down converter performs no better than a phase insensitive amplifier whose internal noise is not squeezed.

In the circuit of Fig. 12(b) the signal is detected in a frequency ω_0 in a band about dc. The signal frequency $\omega_s = \omega_p + \omega_0$ and the image frequency $\omega_i = \omega_p - \omega_0$ both lie in the pass band of the filter on the left port of the mixer. Consider the case when homodyne detection is done at

frequency ω_p ; then, the input in both the signal and image band must be regarded as signal. Under proper impedance matching,

$$\frac{r_s}{r_0} = \frac{\pi^2}{8}, \quad (8.11)$$

one has

$$A_0^{\text{out}}(\omega_0) = \left[\frac{\omega_p + \omega_0}{2\omega_0} \right]^{1/2} A_s^{\text{in}}(\omega_p + \omega_0) - \left[\frac{\omega_p - \omega_0}{2\omega_0} \right]^{1/2} A_i^{\text{in}\dagger}(\omega_p - \omega_0). \quad (8.12)$$

This expression is similar to that given for the degenerate parametric amplifier (5.16). By the absence of noise terms in (8.12) one concludes that noiseless homodyne detection is in principle possible with resistive mixers operating in the quantum regime.

Figure 12(c) shows a frequency down converter for which the image and signal frequency bands are separate. If $r_i = r_s$, then, for the impedance matching condition (8.11), Eq. (8.12) is still valid, but now $A_i^{\text{in}\dagger}$ must be regarded as noise. If instead of terminating the image port with the image resistor r_i one used a squeezed noise termination (as was done for the idler port of the phase insensitive linear amplifier of Fig. 4), then, in analogy to the discussion of Eq. (5.23), the resistive mixer operated as a down converter can noiselessly down convert one quadrature component of the incoming signal.

IX. CONCLUSIONS

A large variety of circuits have been analyzed quantum mechanically in this paper. It is hoped that the following impressions have been generated in the mind of the reader.

(1) For the circuits considered, the full quantum analysis of the circuit is not much more difficult than the classical analysis.

(2) The quantum behavior of complicated lumped circuit networks are worth investigating. From such considerations, noiseless amplifier and mixer configurations, and back-action-evading detectors have been discovered.

(3) The existence of low-noise superconducting devices together with the availability of cryogenic temperatures below 5 mK generated on a routine basis with modern dilution refrigerators makes the exploration of the quantum mechanics of macroscopic devices operating in the microwave and rf frequency range look promising.

ACKNOWLEDGMENTS

Part of the work presented in this paper was carried out during a one month stay at the California Institute of Technology. In this regard we would like to thank Stan Whitcomb and the Gravity Physics Group for their hospitality and support. We especially thank Carlton M. Caves for his helpful discussions. We would also like to thank Jeanne Wilhelm for a critical reading of the manuscript.

- ¹For a historical overview on the works of V. B. Braginsky, R. P. Gifford, W. G. Unruh, C. M. Caves *et al.*, and J. N. Hollenhorst, see K. S. Thorne, C. M. Caves, V. D. Sandberg, M. Zimmermann, and R. W. P. Drever, in *Sources of Gravitational Radiation*, edited by Larry Smarr (Cambridge University Press, London, 1979), p. 49.
- ²C. M. Caves, K. S. Thorne, R. W. P. Drever, V. D. Sandberg, and M. Zimmermann, *Rev. Mod. Phys.* **52**, 341 (1980).
- ³M. B. Ketchen and J. M. Jaycox, *Appl. Phys. Lett.* **40**, 736 (1982).
- ⁴T. G. Phillips, D. P. Woody, G. J. Dolan, R. E. Miller, and R. A. Linke, *IEEE Trans. Magn.* **MAG17**, 684 (1981).
- ⁵A. O. Caldeira and A. J. Leggett, *Phys. Rev. Lett.* **46**, 211 (1981).
- ⁶R. H. Koch, D. J. Van Harlingen, and John Clarke, *Phys. Rev. Lett.* **45**, 2132 (1980).
- ⁷S. Chakravarty, *Bull. Am. Phys. Soc.* **28**, 317 (1983).
- ⁸R. F. Voss and R. A. Webb, *Phys. Rev. Lett.* **47**, 265 (1981).
- ⁹R. H. Koch, D. J. Van Harlingen, and J. Clarke, *Phys. Rev. Lett.* **47**, 1216 (1981).
- ¹⁰L. D. Jackel, J. P. Gordon, E. L. Hu, R. E. Howard, L. A. Fetter, D. M. Tennat, R. W. Epworth, and J. Kurkijärvi, *Phys. Rev. Lett.* **47**, 697 (1981).
- ¹¹H. Nyquist, *Phys. Rev.* **32**, 110 (1928).
- ¹²F. N. H. Robinson, *Noise in Electrical Circuits* (Oxford University Press, London, 1962).
- ¹³W. H. Louisell, *Radiation and Noise in Quantum Electronics* (McGraw-Hill, New York, 1964).
- ¹⁴S. N. Gupta, *Quantum Electrodynamics* (Gordon and Breach, New York, 1977).
- ¹⁵B. Benguira and M. Kac, *Phys. Rev. Lett.* **46**, 1 (1980).
- ¹⁶H. Dekker, *Phys. Rep.* **80**, 1 (1980).
- ¹⁷J. R. Senitzky, *Phys. Rev.* **119**, 670 (1960).
- ¹⁸G. W. Ford, M. Kac, and P. Mazur, *J. Math. Phys.* **6**, 504 (1965).
- ¹⁹M. G. Kendall, *The Advanced Theory of Statistics* (Griffin, London, 1943), Vol. 1.
- ²⁰C. M. Caves, *Phys. Rev. D* **26**, 1817 (1982). See also Ref. 28.
- ²¹H. Takahasi, *Advances in Communication Systems*, edited by A. V. Balakrishnan (Academic, New York, 1965).
- ²²L. A. Blackwell and K. L. Kotzebue, *Semiconductor-Diode Parametric Amplifiers* (Prentice-Hall, Englewood Cliffs, 1961).
- ²³C. M. Caves, *Phys. Rev. Lett.* **45**, 75 (1980).
- ²⁴J. N. Hollenhorst, *Phys. Rev. D* **19**, 1669 (1979).
- ²⁵H. Paul, *Rev. Mod. Phys.* **54**, 1061 (1982).
- ²⁶H. P. Yuen, *Phys. Rev. A* **13**, 2226 (1976).
- ²⁷H. A. Haus and S. A. Mullen, *Phys. Rev.* **128**, 2407 (1962).
- ²⁸B. Yurke and J. Denker, *Physica B* **108**, 1359 (1981).
- ²⁹J. H. Shapiro, *Opt. Lett.* **5**, 351 (1980).
- ³⁰C. Y. Ho, *Microwave J.* **23**, 67 (1980).
- ³¹M. F. Bocko and W. W. Johnson, *Phys. Rev. Lett.* **48**, 1371 (1982).
- ³²J. von Neumann, *Mathematische Grundlagen der Quantenmechanik* (Springer, Berlin, 1932); also B. S. DeWitt, *Phys. Today* **23**, (9), 30 (1970).
- ³³R. P. Feynman and F. L. Vernon, Jr., *Ann. Phys.* **24**, 118 (1963).
- ³⁴A. O. Caldeira and A. J. Leggett, *Ann. Phys.* (to be published).
- ³⁵B. D. Josephson, *Phys. Lett.* **1**, 251 (1962); *Advan. Phys.* **14**, 419 (1965).
- ³⁶P. F. Michelson, Ph.D. thesis, Stanford University, 1979 (unpublished).
- ³⁷S. Rudner and T. Claeson, *J. Appl. Phys.* **50**, 7070 (1979).
- ³⁸H. P. Yuen and J. H. Shapiro, *IEEE Trans. Info. Theory* **IT-26**, 78 (1980).
- ³⁹S. R. Tucker, *IEEE J. Quantum Electron.* **QE-15**, 1234 (1979).
- ⁴⁰A. A. M. Saleh, *Theory of Resistive Mixers* (MIT, Cambridge, Mass., 1971).